5.1 Quantum optics

F. Haug, M. Freyberger, K. Vogel, W.P. Schleich

5.1.1 Introduction

In 1924 Gregor Wentzel – then at the institute of Arnold Sommerfeld in Munich – analyzed [24Wen] the emission and absorption of light by two atoms at different positions. The only quantum theory available to him was the "Atommechanik" à la Bohr–Sommerfeld [25Bor1, 26Pau]. Wentzel was forced to propose a revolutionary idea: Probability amplitudes for the propagation of the light between two points in space are complex-valued phase factors, where the phase is given by the classical action expressed in units of $\hbar$. The path integral formulation of quantum mechanics was born not only before Richard Feynman, but even before quantum mechanics was discovered by Werner Heisenberg and Erwin Schrödinger.

Obviously, Wentzel's paper contains a remarkable approach. However, even more remarkable is the title of his paper: "Zur Quantenoptik", that is "On Quantum Optics". Therefore, Wentzel might well be considered the father of the expression "quantum optics" despite the fact that he used it in a completely different context. Nowadays we interpret the field of quantum optics [89Coh, 91Lou, 91Mey, 92Coh, 94Wal, 95Man, 96Scu, 99Pau, 01Sch] as the domain of optics where quantum mechanics is of importance, that is where the quantization of the radiation field is crucial.

5.1.1.1 A brief history of quantum optics

The electromagnetic field appears almost everywhere in physics. Historically it has played a major role in the development of our understanding of the physical laws of nature. First James Clerk Maxwell [1873Max] in 1864 found the famous system of equations which explains the whole classical realm of electromagnetic field effects. At the beginning of the last century Max Planck initiated quantum theory [1900Pla, 1901Pla] when he discovered the fundamental constant $h \equiv 2\pi\hbar$ in the laws of black-body radiation. In 1905 Albert Einstein explained the photoelectric effect [1905Ein] on the hypothesis of a corpuscular nature of radiation and in 1917 this paradigm helped him to describe the interaction between atoms and electromagnetic radiation introducing the coefficients of spontaneous and induced emission [17Ein].

However, none of this work had been based on a rigorous quantum theory of the electromagnetic field. Such a formalism was put forward later in the paper by Max Born and Pascual Jordan [25Bor3] in which they point out that Heisenberg's non-commuting objects were matrices and in the famous "Drei-Männer-Arbeit" by Born, Heisenberg and Jordan [25Bor2]. Nevertheless, the starting point of quantum optics might well be traced back to the article by Paul Adrian Maurice Dirac [27Dir] in 1927 in which he developed the quantum theory of the emission and absorption of radiation. An independent but equivalent approach was put forward by Enrico Fermi. For a beautiful exposition of the quantum theory of radiation and a wealth of applications we refer to his Ann Arbor summer school contribution [32Fer]. From this theory emerged quantum electrodynamics (QED). It became the role model of all gauge theories of particle physics. In some sense quantum optics is the non-relativistic limit of QED.

In the mid-fifties Robert Hanbury Brown and Richard Twiss – working in the field of radio astronomy – were trying to determine the angular diameters of radio sources. They recognized that in these measurements radiation fluctuations play an essential role. In order to overcome these limitations they developed a new type of intensity interferometer [56Han]. This experiment was performed many years before the laser and represents the starting point for the theory of photon detection and coherence created by Roy J. Glauber at Harvard [63Gla1, 63Gla2].

The development of the laser [83Ber, 99Lam] brought a renaissance to the quantum theory of radiation. Indeed, all the tools of quantum optics were created in the framework of the quantum theory of the laser. Its main proponents were Hermann Haken and his school in Stuttgart [84Hak], Willis E. Lamb and Marlan O. Scully at Yale [74Sar], Melvin Lax [66Lax] and William H. Louisell [73Lou] at Bell Laboratories. Unfortunately, ordinary lasers do not show that many quantum effects. Therefore, the application of theoretical apparatus completed already during the early days of the laser – the high time of quantum electronics – had to wait. For a collection of some of the pioneering papers of this pre-quantum optics era we refer to [70Man].

The detection of photon antibunching [77Kim, 78Kim, 82Cre] and the Mollow-triplet [69Mol] in resonance fluorescence [74Sch, 75Wu, 76Har] ushered in the era of quantum optics. Finally, clean quantum manifestations of the radiation field had been detected and the theoretical tools developed almost 20 years earlier could be put to use. The subsequent observation of squeezed states [85Slu], the development of the one-atom maser [85Mes] and the controlled creation of entangled states capitalizing on the tools of nonlinear optics have emancipated quantum optics. Today it embraces topics such as Bose–Einstein condensation, degenerate fermionic quantum gases, quantum computing, quantum information and quantum communication.

It has become impossible to give a complete overview over the field in a few pages. Therefore, we have decided to concentrate on a few themes that define quantum optics. Space does not allow us to present detailed derivations. Nevertheless we try to outline their logic.

5.1.1.2 Outline of the review

Nowadays we gain more and more insight into the quantum aspects of the electromagnetic field. To this end we must understand the quantization of the field which leads to the concept of a quantum of radiation, the so-called "photon". The name "photon" was coined [95Lam] in 1926 by the chemist Gilbert N. Lewis when he speculated that the transmission of radiation from one atom to another was carried by a new particle [26Lew]. He specifically denied that this particle was Einstein's light quantum. The word "photon" caught on, but not Lewis' meaning. With this motivation in mind we summarize in Sect. 5.1.2 the essential ideas of field quantization in Coulomb gauge.

Specific non-classical features of the electromagnetic field arise for certain quantum states, like squeezed states. Modern quantum optics investigates characteristics which allow us to draw the border line between classical and non-classical field effects. We therefore review in Sect. 5.1.3 important states of radiation fields. Here coherent states play a prominent role since they are the building blocks of Glauber's coherence theory discussed in Sect. 6.1.3 of this volume.

In Sect. 5.1.4 we then turn to the interaction of an atom and a quantized electromagnetic field. Here we focus on the most elementary model of a two-level atom interacting with a single mode of the radiation field. We show how this model describes the experimental realization of photon number states and Schrödinger cat states.

Section 5.1.5 is devoted to a brief introduction into reservoir theory. Here we consider the interaction of a single quantum system – the master system – with a large ensemble of quantum systems which constitute the reservoir. We are only interested in the dynamics of the master system and eliminate the reservoir. This approach allows us to derive the master equation for the damping of a cavity mode which has many applications in the context of decoherence [91Zur, 96Giu] and the emergence of the classical world.

The amazing system of a one-atom maser is the topic of Sect. 5.1.6. In contrast to the familiar laser or maser we achieve in this device microwave amplification by stimulated emission due to a single atom. The emitted radiation displays many non-classical features.

The difference between a classical field and a quantized field manifests itself in the interaction of the radiation field with an atom. A classical field can have zero amplitude. Obviously in this case it does not interact with the atom. On the other hand a quantized field *always* interacts with the atom, even if all the field modes are in their ground states. Then there are still vacuum fluctuations present which lead to various effects such as spontaneous emission and Lamb shift as discussed in Sect. 5.1.7.

The light emitted by a two-level atom driven by a classical field exhibits many interesting features such as photon antibunching and squeezing, as briefly summarized in Sect. 5.1.8.

Section 5.1.9 sketches a few quantum-optical experiments addressing fundamental questions of quantum mechanics. In particular, we review the debate on quantum jumps and discuss the wave–particle duality. We finally turn to the topics of entanglement and experimental verification of Bell inequalities. These tests rely on entangled photon pairs. For a review of other experiments using these unique tools of quantum optics we refer to Sect. 6.1.4.5 of this volume.

We conclude in Sect. 5.1.10 by turning to a few new frontiers of quantum optics. Here we highlight three timely topics: atom optics in quantized fields, Bose–Einstein condensation and quantum information represented by teleportation and quantum cryptography.

5.1.2 Field quantization in Coulomb gauge

In this section we lay the foundations for our review of quantum optics by quantizing the electromagnetic field [89Coh]. We expand the field in a complete set of normal modes which reduces the problem of field quantization to the quantization of a one-dimensional harmonic oscillator corresponding to each normal mode.

5.1.2.1 Mode expansion

The classical free electromagnetic field, that is the field in a region without charge and current densities, obeys the Maxwell equations (see also Vol. VIII/1A1, (1.1.4)–(1.1.7) with (1.1.8)–(1.1.9))

$$\nabla \times \boldsymbol{E} + \frac{\partial \boldsymbol{B}}{\partial t} = 0\,, \qquad \nabla \cdot \boldsymbol{B} = 0\,, \qquad \nabla \times \boldsymbol{H} - \frac{\partial \boldsymbol{D}}{\partial t} = 0\,, \qquad \nabla \cdot \boldsymbol{D} = 0 \tag{5.1.1}$$

expressed in the SI system with $\boldsymbol{B} = \mu_0 \boldsymbol{H}$ and $\boldsymbol{D} = \varepsilon_0 \boldsymbol{E}$. The magnetic permeability μ_0 connects the magnetic induction $\boldsymbol{B}$ with the magnetic field $\boldsymbol{H}$ and the electric permittivity ε_0 of free space connects the displacement $\boldsymbol{D}$ with the electric field $\boldsymbol{E}$. In the case of a free field $\boldsymbol{E}$ and $\boldsymbol{B}$ may be obtained from

$$\boldsymbol{B} = \nabla \times \boldsymbol{A}\,, \quad \boldsymbol{E} = -\frac{\partial \boldsymbol{A}}{\partial t}\,, \tag{5.1.2}$$

where the vector potential $\boldsymbol{A}$ obeys the Coulomb gauge condition $\nabla \cdot \boldsymbol{A} = 0$ and satisfies a wave equation.

Due to the linear structure of Maxwell's equations we can decompose the vector potential into normal modes according to

$$\boldsymbol{A}(\boldsymbol{r},t) = \sum_{\ell} \left(\frac{\hbar}{2\Omega_\ell \varepsilon_0 V_\ell} \right)^{1/2} \left(\boldsymbol{u}_\ell(\boldsymbol{r}) \alpha_\ell \mathrm{e}^{-\mathrm{i}\Omega_\ell t} + \mathrm{c.c.} \right) \tag{5.1.3}$$

with complex mode amplitudes α_ℓ.

The mode functions $\boldsymbol{u}_\ell(\boldsymbol{r})$ are solutions of the Helmholtz equation

$$\Delta \boldsymbol{u}_\ell(\boldsymbol{r}) + \frac{\Omega_\ell^2}{c^2} \boldsymbol{u}_\ell(\boldsymbol{r}) = 0 \tag{5.1.4}$$

with the mode frequencies Ω_ℓ and the speed of light c. They have to fulfill the Coulomb gauge $\nabla \cdot \boldsymbol{u}_\ell = 0$. We choose $\boldsymbol{u}_\ell$ to be dimensionless and scale it such that the maximum of $|\boldsymbol{u}_\ell|^2$ is one. This choice allows us to define the effective mode volume V_ℓ of the mode ℓ via the orthogonality relation

$$\int \mathrm{d}V \boldsymbol{u}_\ell^*(\boldsymbol{r}) \boldsymbol{u}_{\ell'}(\boldsymbol{r}) = \delta_{\ell,\ell'} V_\ell \,. \tag{5.1.5}$$

Here we integrate over the region of space where the electromagnetic field and therefore $\boldsymbol{u}_\ell$ is non-zero. The frequencies Ω_ℓ of the modes ℓ follow from the boundary conditions for $\boldsymbol{u}_\ell$. We consider two cases: running waves in free space and standing waves in a ideal resonator.

5.1.2.1.1 Running waves

We start by discussing periodic boundary conditions for the mode functions $\boldsymbol{u}_\ell$ in the quantization volume V. In this case we can solve the Helmholtz equation (5.1.4) in terms of plane waves. Therefore, with these mode functions the vector potential reads

$$\boldsymbol{A}(\boldsymbol{r},t) = \sum_{\boldsymbol{k}} \sum_{\sigma=1}^{2} \left(\frac{\hbar}{2\Omega_{\boldsymbol{k}} \varepsilon_0 V} \right)^{1/2} \left(\alpha_{\boldsymbol{k}\sigma} \boldsymbol{\epsilon}_{\boldsymbol{k}\sigma} \mathrm{e}^{\mathrm{i}(\boldsymbol{k}\cdot\boldsymbol{r} - \Omega_{\boldsymbol{k}} t)} + \mathrm{c.c.} \right) , \tag{5.1.6}$$

where the effective volume V_ℓ of each mode is identical to the quantization volume V.

Instead of the index ℓ we now use a wave vector $\boldsymbol{k}$ and two polarization vectors $\boldsymbol{\epsilon}_{\boldsymbol{k}1}$ and $\boldsymbol{\epsilon}_{\boldsymbol{k}2}$ to characterize the modes. The gauge condition $\nabla \cdot \boldsymbol{A} = 0$ implies that these polarization vectors have to be orthogonal to the wave vector $\boldsymbol{k}$, that is $\boldsymbol{\epsilon}_{\boldsymbol{k}1} \cdot \boldsymbol{k} = \boldsymbol{\epsilon}_{\boldsymbol{k}2} \cdot \boldsymbol{k} = 0$ for each wave vector $\boldsymbol{k}$. The frequencies $\Omega_{\boldsymbol{k}}$ are related to the wave vectors $\boldsymbol{k}$ via the dispersion relation $\Omega_{\boldsymbol{k}} = c|\boldsymbol{k}|$. The periodicity condition leads to a discrete set of wave vectors $\boldsymbol{k} \equiv 2\pi/V^{1/3}(n_x, n_y, n_z)$, where $n_x, n_y, n_z = 0, \pm 1, \pm 2 \ldots$. The Fourier amplitudes $\alpha_{\boldsymbol{k}\sigma}$ are complex numbers in the classical theory.

With the help of (5.1.2) we can decompose $\boldsymbol{E}$ and $\boldsymbol{B}$ into normal modes and find

$$\boldsymbol{E}(\boldsymbol{r},t) = \mathrm{i} \sum_{\boldsymbol{k}} \sum_{\sigma=1}^{2} \left(\frac{\hbar \Omega_{\boldsymbol{k}}}{2\varepsilon_0 V} \right)^{1/2} \left(\alpha_{\boldsymbol{k}\sigma} \boldsymbol{\epsilon}_{\boldsymbol{k}\sigma} \mathrm{e}^{\mathrm{i}(\boldsymbol{k}\cdot\boldsymbol{r} - \Omega_{\boldsymbol{k}} t)} - \mathrm{c.c.} \right) \tag{5.1.7}$$

for the electric field and a similar expression for the magnetic induction $\boldsymbol{B}$.

5.1.2.1.2 Standing waves

In the context of cavity QED the mode functions are determined by the resonator. At the boundary of an ideal cavity the tangential component of the electric field $\boldsymbol{E}$ and the normal component of the magnetic induction $\boldsymbol{B}$ have to vanish. Both conditions are fulfilled when the tangential component of each mode function $\boldsymbol{u}_\ell$ vanishes at the boundary of the resonator. For open resonators we require in addition that the electromagnetic field and therefore $\boldsymbol{u}_\ell$ vanishes at infinity. These boundary conditions determine the frequency Ω_ℓ of the mode ℓ. Furthermore, it is convenient to use real mode functions $\boldsymbol{u}_\ell$. For the vector potential we then find

$$\boldsymbol{A}(\boldsymbol{r},t) = \sum_\ell \left(\frac{\hbar}{2\Omega_\ell \varepsilon_0 V_\ell}\right)^{1/2} \boldsymbol{u}_\ell(\boldsymbol{r}) \left(\alpha_\ell \mathrm{e}^{-\mathrm{i}\Omega_\ell t} + \text{c.c.}\right) \tag{5.1.8}$$

and the electric field takes the form

$$\boldsymbol{E}(\boldsymbol{r},t) = \mathrm{i} \sum_\ell \left(\frac{\hbar\Omega_\ell}{2\varepsilon_0 V_\ell}\right)^{1/2} \boldsymbol{u}_\ell(\boldsymbol{r}) \left(\alpha_\ell \mathrm{e}^{-\mathrm{i}\Omega_\ell t} - \text{c.c.}\right) . \tag{5.1.9}$$

From (5.1.2) we find a similar relation for the magnetic induction $\boldsymbol{B}$.

5.1.2.1.3 Energy of the radiation field

With the help of (5.1.9) for the electric field and the analogous expression for the magnetic field we can express the field energy

$$H_\mathrm{f} \equiv \frac{1}{2} \int \mathrm{d}V \left(\varepsilon_0 \boldsymbol{E}^2(\boldsymbol{r},t) + \boldsymbol{B}^2(\boldsymbol{r},t)/\mu_0\right) \tag{5.1.10}$$

in terms of the mode amplitudes α_ℓ and α_ℓ^* and arrive at

$$H_\mathrm{f} = \sum_\ell \frac{\hbar\Omega_\ell}{2} \left(\alpha_\ell \alpha_\ell^* + \alpha_\ell^* \alpha_\ell\right) , \tag{5.1.11}$$

where we have already anticipated that in the next section the mode amplitudes become non-commuting operators.

5.1.2.2 Field quantization

The mode decomposition of the electromagnetic field discussed in the previous sections allows us to quantize the field. In the Schrödinger picture we have to replace the time-dependent amplitudes $\alpha_\ell \mathrm{e}^{-\mathrm{i}\Omega_\ell t}$ by the time-independent mode annihilation operators $\hat{a}_\ell$. The complex conjugates $\alpha_\ell^* \mathrm{e}^{\mathrm{i}\Omega_\ell t}$ are replaced by the time-independent mode creation operators $\hat{a}_\ell^\dagger$. These operators obey the commutation relations

$$[\hat{a}_\ell, \hat{a}_{\ell'}^\dagger] = \delta_{\ell\ell'} . \tag{5.1.12}$$

The representations of the vector potential, the electric field and the magnetic induction in terms of these operators follows from (5.1.6)–(5.1.9). For running waves we find

$$\hat{\boldsymbol{A}}(\boldsymbol{r}) = \sum_{\boldsymbol{k}} \sum_{\sigma=1}^{2} \left(\frac{\hbar}{2\varepsilon_0 \Omega_{\boldsymbol{k}} V}\right)^{1/2} \left(\hat{a}_{\boldsymbol{k}\sigma} \boldsymbol{\epsilon}_{\boldsymbol{k}\sigma} \mathrm{e}^{\mathrm{i}\boldsymbol{k}\cdot\boldsymbol{r}} + \text{h.c.}\right) , \tag{5.1.13}$$

$$\hat{\boldsymbol{E}}(\boldsymbol{r}) = \mathrm{i} \sum_{\boldsymbol{k}} \sum_{\sigma=1}^{2} \left(\frac{\hbar\Omega_{\boldsymbol{k}}}{2\varepsilon_0 V}\right)^{1/2} \left(\hat{a}_{\boldsymbol{k}\sigma} \boldsymbol{\epsilon}_{\boldsymbol{k}\sigma} \mathrm{e}^{\mathrm{i}\boldsymbol{k}\cdot\boldsymbol{r}} - \text{h.c.}\right) \equiv \hat{\boldsymbol{E}}^+(\boldsymbol{r}) + \hat{\boldsymbol{E}}^-(\boldsymbol{r}) , \tag{5.1.14}$$

whereas for standing waves we have

$$\hat{\boldsymbol{A}}(\boldsymbol{r}) = \sum_{\ell} \left(\frac{\hbar}{2\varepsilon_0 \Omega_\ell V_\ell} \right)^{1/2} \boldsymbol{u}_\ell(\boldsymbol{r}) \left(\hat{a}_\ell + \hat{a}_\ell^\dagger \right) , \tag{5.1.15}$$

$$\hat{\boldsymbol{E}}(\boldsymbol{r}) = \mathrm{i} \sum_{\ell} \left(\frac{\hbar \Omega_\ell}{2\varepsilon_0 V_\ell} \right)^{1/2} \boldsymbol{u}_\ell(\boldsymbol{r}) \left(\hat{a}_\ell - \hat{a}_\ell^\dagger \right) \equiv \hat{\boldsymbol{E}}^+(\boldsymbol{r}) + \hat{\boldsymbol{E}}^-(\boldsymbol{r}) . \tag{5.1.16}$$

In the last step we have decomposed the electric field operator into the positive and negative frequency parts $\hat{\boldsymbol{E}}^+$ and $\hat{\boldsymbol{E}}^-$, respectively. A similar relation holds for the operator describing the magnetic induction $\hat{\boldsymbol{B}}$.

The expression (5.1.11) for the field energy and the commutation relations (5.1.12) allow us to write the Hamiltonian

$$\hat{H}_\mathrm{f} = \sum_{\ell} \hbar \Omega_\ell (\hat{a}_\ell^\dagger \hat{a}_\ell + 1/2) \tag{5.1.17}$$

as a sum of independent harmonic oscillator Hamiltonians corresponding to each mode ℓ.

5.1.2.3 Single mode

Since normal modes are independent from each other, we can often restrict the discussion to a single mode and suppress the mode index ℓ. The corresponding Hamiltonian then reads

$$\hat{H}_\mathrm{f} = \hbar \Omega (\hat{a}^\dagger \hat{a} + 1/2) = \hbar \Omega \left(\frac{1}{2} \hat{p}^2 + \frac{1}{2} \hat{x}^2 \right) , \tag{5.1.18}$$

where the quadrature operators

$$\hat{x} \equiv \frac{1}{\sqrt{2}} (\hat{a} + \hat{a}^\dagger) \quad \text{and} \quad \hat{p} \equiv \frac{1}{\mathrm{i}\sqrt{2}} (\hat{a} - \hat{a}^\dagger) \tag{5.1.19}$$

are equivalent to scaled position and momentum operators $\hat{x}$ and $\hat{p}$ of a massive particle in a harmonic potential. Since they obey the commutation relation $[\hat{x}, \hat{p}] = \mathrm{i}$, their uncertainties $(\Delta x)^2 \equiv \langle \hat{x}^2 \rangle - \langle \hat{x} \rangle^2$ and $(\Delta p)^2 \equiv \langle \hat{p}^2 \rangle - \langle \hat{p} \rangle^2$ fulfill the Heisenberg inequality $\Delta x \Delta p \geq 1/2$.

We conclude by emphasizing that the quantum nature of the electromagnetic field enters through the amplitude operators $\hat{a}_\ell$ and $\hat{a}_\ell^\dagger$. It is therefore not surprising that the components of the electric and the magnetic field do not commute. As a consequence they cannot be measured simultaneously with arbitrary accuracy. The uncertainty relations for the electric and magnetic field components were derived for the first time by Niels Bohr and Léon Rosenfeld [33Boh, 50Boh]. For a more detailed discussion we refer to [73Lou].

5.1.3 Field states

When we quantize a system the step of representing observables by operators is only one side of the coin. To describe the state of the system by a quantum state constitutes the other side.

In this section we briefly summarize important properties of several states of the electromagnetic field. Space does not allow us to go into great detail nor can we do justice to the wealth of quantum states. For our review we have chosen number states, coherent states, squeezed states and thermal states. For a more complete treatment we refer to the literature [91Mey, 94Wal, 95Man, 96Scu, 01Sch]. For a discussion of unusual states such as phase states we recommend [68Car, 89Peg, 93Sch]. In later sections we describe how these states have been created in experiments.

Before we discuss those states in detail we briefly review the state concept of quantum mechanics.

5.1.3.1 Pure and mixed states

The state vector $|\,\psi\,\rangle$ contains the full information about a quantum system. However, in many cases we do not know every detail of our system. This lack of information could be for example because the system has too many degrees of freedom. Another reason could be due to the fact that our system is coupled to a reservoir and we cannot keep track of the motion of the individual constituents. A damped cavity field, discussed in Sect. 5.1.5, or an atom that undergoes spontaneous emission, analyzed in Sect. 5.1.7, represent two such systems coupled to a reservoir. In both cases we cannot describe the system by a state vector but by a density operator.

The density operator $\hat{\rho}$ of a pure state $|\,\psi\,\rangle$ reads

$$\hat{\rho} \equiv |\,\psi\,\rangle\langle\,\psi\,|\,. \tag{5.1.20}$$

A mixed state is an incoherent superposition

$$\hat{\rho} = \sum_n W_n |\,\psi_n\,\rangle\langle\,\psi_n\,| \tag{5.1.21}$$

of pure states $|\,\psi_n\,\rangle$ with probabilities W_n such that $\sum_n W_n = 1$.

The expectation value $\langle\hat{\mathcal{O}}\rangle$ of the observable $\hat{\mathcal{O}}$ then involves two averages, namely the quantum-mechanical average $\langle\,\psi_n\,|\,\hat{\mathcal{O}}\,|\,\psi_n\,\rangle$ and the one over the statistics W_n of the states $|\,\psi_n\,\rangle$, that is

$$\langle\hat{\mathcal{O}}\rangle = \sum_n W_n \langle\,\psi_n\,|\,\hat{\mathcal{O}}\,|\,\psi_n\,\rangle = \mathrm{Tr}\left(\hat{\mathcal{O}}\hat{\rho}\right)\,. \tag{5.1.22}$$

In the last step we have introduced the operation $\mathrm{Tr}\,\hat{A} \equiv \sum_i \langle\,i\,|\,\hat{A}\,|\,i\,\rangle$ of the trace of an operator $\hat{A}$, where we sum over an arbitrary complete set of states $|\,i\,\rangle$.

In the language of the trace the normalization condition of the probabilities W_n reads $\mathrm{Tr}\,\hat{\rho} = 1$. Moreover, we find the inequality

$$\mathrm{Tr}\,\hat{\rho}^{\,2} \leq 1\,. \tag{5.1.23}$$

Since the equal sign arises only for pure states, the calculation of $\mathrm{Tr}\,\hat{\rho}^{\,2}$ allows to identify a pure state from the density operator.

5.1.3.2 Photon number states

We start our walk through the gallery of single-mode field states by considering the eigenstates $|\,n\,\rangle$ of the number operator $\hat{n} \equiv \hat{a}^\dagger\hat{a}$. The corresponding eigenvalue equation reads

$$\hat{n}|\,n\,\rangle = \hat{a}^\dagger\hat{a}|\,n\,\rangle = n|\,n\,\rangle\,, \tag{5.1.24}$$

where $n = 0, 1, 2, \ldots$ denotes the number of excitations or the number of photons in the mode. The states $|\,n\,\rangle$ also carry the name Fock states.

The state $|\,0\,\rangle$, that is the vacuum state of the mode, is defined by $\hat{a}|\,0\,\rangle = 0$. We can climb the ladder of excitations up and down via the application of the creation and the annihilation operators $\hat{a}^\dagger$ and $\hat{a}$ on a Fock state $|\,n\,\rangle$ which yields

$$\hat{a}^\dagger|\,n\,\rangle = \sqrt{n+1}\;\;|\,n+1\,\rangle, \quad \hat{a}|\,n\,\rangle = \sqrt{n}\;\;|\,n-1\,\rangle\,. \tag{5.1.25}$$

Number states form a complete and orthonormal set of states and therefore provide the frequently used representation

$$|\,\psi\,\rangle = \sum_{n=0}^{\infty}\langle\,n\,|\,\psi\,\rangle|\,n\,\rangle \equiv \sum_{n=0}^{\infty}\psi_n|\,n\,\rangle \tag{5.1.26}$$

of a pure quantum state $|\,\psi\,\rangle$, or a mixed quantum state

$$\hat{\rho} = \sum_{m,n=0}^{\infty}\langle\,m\,|\hat{\rho}\,|\,n\,\rangle|\,m\,\rangle\langle\,n\,| \equiv \sum_{m,n=0}^{\infty}\rho_{mn}|\,m\,\rangle\langle\,n\,| \tag{5.1.27}$$

described by a density operator $\hat{\rho}$.

In Sect. 5.1.4.3 we briefly describe an experiment that has created in a controlled way photon number states in a cavity. A different method uses the photon pair in two-photon down conversion [99Zei].

5.1.3.3 Coherent states

In an attempt to show that there exist non-spreading wave packets in quantum mechanics Erwin Schrödinger [26Sch2] in 1926 studied the time evolution of a displaced ground state of a harmonic oscillator. He found that indeed the Gaussian probability density of the wave packet maintains its shape. In the concluding sentences of his paper he even expresses his optimism that similar wave packets may also be found for the hydrogen atom. Unfortunately, no such states exist since the spectrum of the hydrogen atom is not equidistant.

Almost 40 years later, Roy J. Glauber [63Gla1, 63Gla2] revisited these special states which he called “coherent states”. They are the building blocks for the formalism of photon detection and coherence theory. For a summary of these topics we refer to [65Gla].

According to Glauber a coherent state $|\,\alpha\,\rangle$ is an eigenstate of the annihilation operator

$$\hat{a}|\,\alpha\,\rangle = \alpha|\,\alpha\,\rangle \tag{5.1.28}$$

with the complex amplitude $\alpha \equiv |\alpha|\mathrm{e}^{\mathrm{i}\theta}$.

An alternative representation of a coherent state is by the action of the displacement operator $\hat{D}(\alpha)$ on the vacuum, that is

$$|\,\alpha\,\rangle \equiv \mathrm{e}^{\alpha\hat{a}^\dagger-\alpha^*\hat{a}}|\,0\,\rangle \equiv \hat{D}(\alpha)|\,0\,\rangle = \mathrm{e}^{-|\alpha|^2/2}\sum_{n=0}^{\infty}\frac{\alpha^n}{\sqrt{n!}}|\,n\,\rangle\,. \tag{5.1.29}$$

Hence, the photon distribution

$$W_n \equiv |\langle\,n\,|\,\alpha\,\rangle|^2 = \frac{|\alpha|^{2n}\mathrm{e}^{-|\alpha|^2}}{n!} \tag{5.1.30}$$

of a coherent state is a Poisson distribution with average photon number $\langle\hat{n}\rangle = |\alpha|^2$ and variance $(\Delta n)^2 \equiv \langle\hat{n}^2\rangle - \langle\hat{n}\rangle^2 = |\alpha|^2$. Consequently, the relative fluctuations $(\Delta n)/\langle\hat{n}\rangle = \langle\hat{n}\rangle^{-1/2}$ vanish for a large average photon number.

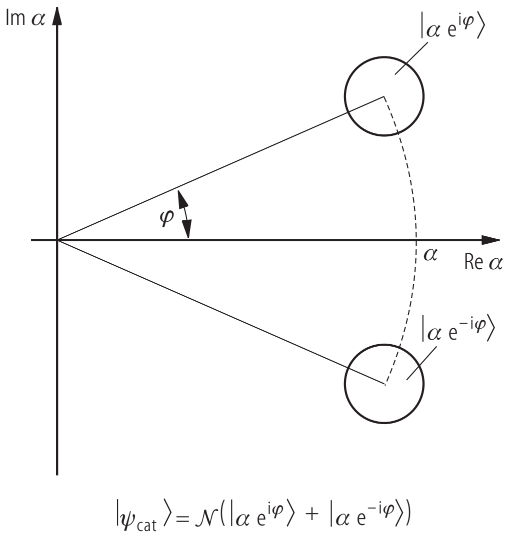

Fig. 5.1.1. In its most elementary version the quantum-mechanical superposition of two coherent states of average photon number $\langle \hat{n} \rangle = \alpha^2$ and phase difference 2φ can be visualized by two circles of radius unity displaced by an amount α from the origin and having the angle φ between them and the real axis.

A coherent state is an eigenstate of $\hat{a}$. However, a superposition [91Sch]

$$|\,\psi_{\text{cat}}\,\rangle \equiv \mathcal{N}\,\left[|\,\alpha e^{i\varphi}\,\rangle + |\,\alpha e^{-i\varphi}\,\rangle\right] \tag{5.1.31}$$

of two coherent states of identical real-valued amplitudes α but different phases φ and $-\varphi$ depicted in Fig. 5.1.1 is not an eigenstate of $\hat{a}$. Such a state with an appropriate normalization factor $\mathcal{N}$ is an example of a so-called Schrödinger cat state which was first introduced in Schrödinger's metaphor [35Sch].

In Sect. 5.1.4.3 we discuss a cavity QED experiment and mention an ion trap experiment which describes the preparation of such a state. Moreover, in Sect. 5.1.5.3 we explain why these states provide deeper insight into the emergence of the classical world from quantum mechanics.

5.1.3.4 Squeezed states

We obtain a squeezed state $|\,\alpha,\epsilon\,\rangle$ by applying the displacement operator $\hat{D}(\alpha)$ and the unitary squeeze operator

$$\hat{S}(\epsilon) \equiv e^{\frac{1}{2}\epsilon^*\hat{a}^2 - \frac{1}{2}\epsilon\hat{a}^{\dagger 2}} \tag{5.1.32}$$

with $\epsilon \equiv r e^{-2i\phi}$ to the vacuum

$$|\,\alpha,\epsilon\,\rangle \equiv \hat{D}(\alpha)\hat{S}(\epsilon)|\,0\,\rangle\,. \tag{5.1.33}$$

The nature of squeezed states stands out in the uncertainties $(\Delta X_1)^2 \equiv \langle \hat{X}_1^2\rangle - \langle \hat{X}_1\rangle^2$ and $(\Delta X_2)^2 \equiv \langle \hat{X}_2^2\rangle - \langle \hat{X}_2\rangle^2$ for the rotated quadratures

$$\hat{X}_1 \equiv \hat{x}\,\cos\phi - \hat{p}\,\sin\phi\,, \quad \hat{X}_2 \equiv \hat{p}\,\cos\phi + \hat{x}\,\sin\phi\,, \tag{5.1.34}$$

where the ordinary quadrature operators $\hat{x}$ and $\hat{p}$ are defined in (5.1.19). Indeed, we find

$$\Delta X_1 = e^{-r}/\sqrt{2}\,, \quad \Delta X_2 = e^{r}/\sqrt{2}\,. \tag{5.1.35}$$

A squeezed state is a minimum uncertainty state since the product $\Delta X_1 \cdot \Delta X_2 = 1/2$ saturates the Heisenberg uncertainty relation. For $r = 0$ we have a coherent state. In this case the two

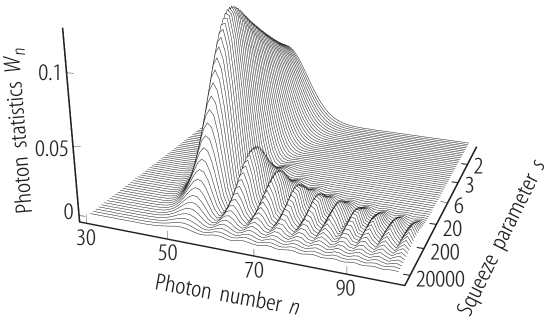

Fig. 5.1.2. Photon statistics W_n of a squeezed state for different choices of the squeeze parameter $s \equiv \mathrm{e}^r$. All curves are plotted for the same value $\alpha = 7$ of the displacement parameter. The rearmost curve (no squeezing at all, $s = 1$) shows the ideal Poisson distribution associated with a coherent state. Curves that are further forward display oscillations in the photon statistics.

uncertainties $\Delta X_1 = \Delta X_2 = 1/\sqrt{2}$ are equal. However, for $r \neq 0$ the fluctuations in one quadrature are squeezed at the expense of the other. For $r > 0$ the fluctuations in the variable X_1 are squeezed, whereas for $r < 0$ the fluctuations in X_2 are squeezed. The angle ϕ indicates a rotation of the coordinate system. For $\phi = 0$ the squeezed state $|\,\alpha, r\,\rangle$ is a minimum uncertainty state for the quadratures $\hat{x}$ and $\hat{p}$ with $\Delta x = \mathrm{e}^{-r}/\sqrt{2}$ and $\Delta p = \mathrm{e}^{r}/\sqrt{2}$.

The photon number distribution $W_n \equiv |\langle\,\alpha, r\,|\,n\,\rangle|^2$ can be narrower or broader than the one for the corresponding coherent state with the same α. This narrowing of the photon distribution, that is the sub-Poissonian behavior, is one of the non-classical features of a squeezed state. Furthermore, W_n displays oscillations [87Sch] for larger squeezing as shown in Fig. 5.1.2.

Several experiments have demonstrated the generation of squeezed light making use of nonlinear optics. For more details we refer to the special issues [87Kim, 87Lou, 92Gia].

5.1.3.5 Thermal states

The most elementary example of a density operator $\hat{\rho}$ is that of a thermal state for an oscillator with frequency Ω. This density operator corresponds to a state for which we only know that it obeys a Boltzmann photon statistics $W_n = (1 - \mathrm{e}^{-\beta})\,\mathrm{e}^{-n\beta}$, where $\beta \equiv \hbar\Omega/(k_\mathrm{B}T)$. Here k_B and T denote the Boltzmann constant and the temperature corresponding to the thermal state, respectively. In this case the density operator reads

$$\hat{\rho}_\mathrm{th} \equiv \sum_{n=0}^{\infty} W_n |\,n\,\rangle\langle\,n\,| = (1 - \mathrm{e}^{-\beta}) \sum_{n=0}^{\infty} \mathrm{e}^{-n\beta} |\,n\,\rangle\langle\,n\,|\,. \tag{5.1.36}$$

The parameter β and therefore the temperature T is intimately related to the average number of thermal photons

$$n_\mathrm{th} = \mathrm{Tr}\,(\hat{n}\hat{\rho}_\mathrm{th}) = \sum_{n=0}^{\infty} n W_n = \frac{\mathrm{e}^{-\beta}}{1 - \mathrm{e}^{-\beta}} = \frac{1}{\exp\left(\frac{\hbar\Omega}{k_\mathrm{B}T}\right) - 1}\,. \tag{5.1.37}$$

When we express the Boltzmann factor $\mathrm{e}^{-\beta}$ by n_th we find the expression

$$\hat{\rho}_\mathrm{th} = \frac{1}{n_\mathrm{th} + 1} \sum_{n=0}^{\infty} \left(\frac{n_\mathrm{th}}{n_\mathrm{th} + 1}\right)^n |\,n\,\rangle\langle\,n\,| \tag{5.1.38}$$

for the density operator of a thermal state.

5.1.3.6 Measures of non-classicality

One of our goals in this review is to highlight physical effects originating from the quantization of the radiation field. For this purpose we focus on states that cannot be described by a classical field.

5.1.3.6.1 Mandel Q-parameter

A convenient indicator of a non-classical field is the Mandel Q-parameter [95Man]

$$Q \equiv \frac{(\Delta n)^2 - \langle \hat{n} \rangle}{\langle \hat{n} \rangle} \equiv \sigma - 1\,, \tag{5.1.39}$$

which is closely related to the normalized variance $\sigma \equiv (\Delta n)^2/\langle \hat{n} \rangle$ of the photon distribution.

For a coherent state we find with $\langle \hat{n} \rangle = \alpha^2$ and $(\Delta n)^2 = \alpha^2$ the Mandel parameter $Q = 0$. A field in a coherent state is considered to be closest to a classical field since it saturates the Heisenberg uncertainty relation and has the same uncertainty in each quadrature component. Therefore, $Q = 0$ defines a boundary between a classical and a quantum field. Indeed, for a thermal state we find $(\Delta n)^2 = n_{\mathrm{th}}^2 + n_{\mathrm{th}}$, corresponding to a photon distribution broader than a Poissonian and hence $Q = n_{\mathrm{th}} > 0$. For $Q < 0$ the photon distribution becomes narrower than that of a Poissonian. The corresponding state is non-classical. The most elementary examples of non-classical states are number states. Since they are eigenstates of the photon number operator $\hat{n}$ the fluctuations in $\hat{n}$ vanish and the Mandel Q-parameter reads $Q = -1$. A squeezed state can display a photon distribution that is either broader or narrower than a Poissonian leading a Mandel Q-parameter that is either positive or negative.

5.1.3.6.2 Glauber–Sudarshan distribution

Another indicator of a non-classical field state is the Glauber–Sudarshan distribution P. It arises in the expansion of the density operator into coherent states. Indeed, coherent states form an over-complete set. Hence states and operators can be expanded into coherent states. In particular, the density operator $\hat{\rho}$ can be expressed in the diagonal form

$$\hat{\rho} = \int \mathrm{d}^2\alpha\, P(\alpha) |\, \alpha \,\rangle\langle\, \alpha \,|\,, \tag{5.1.40}$$

where $P(\alpha)$ denotes the Glauber–Sudarshan phase space distribution [63Gla1, 63Gla2, 63Sud].

For a coherent state $|\,\alpha_0\,\rangle$ the P-distribution is obviously a Dirac delta function located at $\alpha = \alpha_0$, that is $P_{|\,\alpha_0\,\rangle} = \delta(\alpha - \alpha_0)$. In contrast, we find for a thermal state a Gaussian P-distribution, that is $P_{\mathrm{th}}(\alpha) = (\pi\, n_{\mathrm{th}})^{-1} \exp[-|\alpha|^2/n_{\mathrm{th}}]$ which is no longer singular. However, the P-distributions of a number state or a squeezed state are highly singular. They either involve a finite or an infinite number of derivatives of a delta function. Therefore, similar to the Mandel Q-parameter the Dirac delta function P-distribution of the coherent state defines a possible border between classical and quantum field states.

5.1.4 Atom–field interaction

So far, we have only considered the properties of the radiation field. In the present section we couple this quantized field to an atom. We therefore add more quantum degrees of freedom to our system. Indeed, we now have also to take into account the internal states of the atom as well as its center-of-mass motion. In this review we only motivate how to construct the appropriate interaction between these three quantum degrees and refer for a detailed derivation to the literature [01Sch].

5.1.4.1 Electric field–dipole interaction

An optical field does not change considerably over the size of an atom. Hence, the electric field $\boldsymbol{E}$ at the position $\boldsymbol{r}_{\mathrm{e}}$ of the valence electron is almost identical to the electric field at the position $\boldsymbol{r}_{\mathrm{p}}$ of the positively charged rest atom or to the one at the center-of-mass $\boldsymbol{R}$. Therefore, we can make the dipole approximation in which the potential energy reads

$$H_{\boldsymbol{r}\cdot\boldsymbol{E}} \equiv -\wp \cdot \boldsymbol{E}(\boldsymbol{R},t) = -e\boldsymbol{r}\cdot\boldsymbol{E}(\boldsymbol{R},t)\,. \tag{5.1.41}$$

Here we have introduced the electric dipole moment $\wp = e\boldsymbol{r} = e(\boldsymbol{r}_{\mathrm{e}} - \boldsymbol{r}_{\mathrm{p}})$ of an electron with charge e and the rest atom.

The total Hamiltonian of the atom in the electromagnetic field in dipole approximation then reads

$$\widetilde{H} \equiv H_{\mathrm{f}} + H_{\mathrm{cm}} + H_{\mathrm{at}} + H_{\boldsymbol{r}\cdot\boldsymbol{E}} \equiv H_{\mathrm{f}} + \frac{\boldsymbol{P}^2}{2M} + \frac{\boldsymbol{p}^2}{2\mu} + V(\boldsymbol{r}) - e\boldsymbol{r}\cdot\boldsymbol{E}(\boldsymbol{R},t)\,, \tag{5.1.42}$$

where H_{f} is the Hamiltonian of the radiation field (see (5.1.10)) and M and μ are the total and the reduced mass of the two parts of the atom. Moreover, we have introduced the momenta $\boldsymbol{P}$ and $\boldsymbol{p}$ of the center-of-mass and the relative motion, respectively. The interaction between valence electron and rest atom is represented by the potential $V(\boldsymbol{r})$.

In the quantum version of this Hamiltonian we have to replace all observables by operators. We identify three quantum degrees of freedom: (i) the center-of-mass motion described by the conjugate variables $\hat{\boldsymbol{R}}$ and $\hat{\boldsymbol{P}}$ with commutation relation $[\hat{R}_j, \hat{P}_k] = \mathrm{i}\hbar\delta_{jk}$; (ii) the relative motion described by the Hamiltonian $\hat{H}_{\mathrm{at}} \equiv \hat{\boldsymbol{p}}^2/(2\mu) + V(\hat{\boldsymbol{r}})$ which contains the conjugate variables $\hat{\boldsymbol{r}}$ and $\hat{\boldsymbol{p}}$ with commutation relation $[\hat{r}_j, \hat{p}_k] = \mathrm{i}\hbar\delta_{jk}$; and (iii) the electric field operator $\hat{\boldsymbol{E}}$. The interaction Hamiltonian $\hat{H}_{\boldsymbol{r}\cdot\boldsymbol{E}}$ couples all three degrees of freedom.

We emphasize that for many applications this Hamiltonian suffices. However, this ad hoc procedure can also lead to inconsistent results as discussed in [94Wil].

5.1.4.2 Simple model for atom–field interaction

The most elementary model of the interaction of an atom with a quantized electromagnetic field consists of a two-level atom and a single mode of the cavity field. This model still contains enough physics to describe most phenomena in cavity QED and atom optics. When we neglect the center-of-mass motion, that is consider only the interaction between the quantized cavity field and the two levels we call this model the Jaynes–Cummings–Paul model [63Jay, 63Pau].

5.1.4.2.1 Hamiltonian

For the description of the internal dynamics of a two-level atom with excited state $|\,a\,\rangle$ and ground state $|\,b\,\rangle$ separated by an energy $\hbar\omega$ we recall the Pauli operators

$$\hat{\sigma} \equiv \frac{1}{2}\left(\hat{\sigma}_x - \mathrm{i}\hat{\sigma}_y\right) \equiv |\,b\,\rangle\langle\,a\,|\,, \quad \hat{\sigma}^\dagger \equiv \frac{1}{2}\left(\hat{\sigma}_x + \mathrm{i}\hat{\sigma}_y\right) \equiv |\,a\,\rangle\langle\,b\,|\,, \quad \hat{\sigma}_z \equiv |\,a\,\rangle\langle\,a\,| - |\,b\,\rangle\langle\,b\,|\,. \tag{5.1.43}$$

They allow us to represent the Hamiltonian $\hat{H}_{\mathrm{at}} = \hbar\omega\,\hat{\sigma}_z/2$ of the atom and the transitions $\hat{\sigma}|\,a\,\rangle = |\,b\,\rangle$ and $\hat{\sigma}^\dagger|\,b\,\rangle = |\,a\,\rangle$ between the two levels in the energy eigenbasis. In this basis the atomic dipole operator $\hat{\boldsymbol{\wp}} = e\hat{\boldsymbol{r}}$ takes the form $\hat{\boldsymbol{\wp}} = \boldsymbol{\wp}\,\hat{\sigma}^\dagger + \boldsymbol{\wp}^*\,\hat{\sigma}$, where $\boldsymbol{\wp}$ is given by $\boldsymbol{\wp} \equiv e\,\langle\,a\,|\,\hat{\boldsymbol{r}}\,|\,b\,\rangle$. Please note, that the diagonal elements $\langle\,a\,|\,\hat{\boldsymbol{r}}\,|\,a\,\rangle$ and $\langle\,b\,|\,\hat{\boldsymbol{r}}\,|\,b\,\rangle$ vanish due to parity.

The electric field operator (5.1.16) of a single cavity mode characterized by a mode function $\boldsymbol{u}(\hat{\boldsymbol{R}})$, a mode frequency Ω and mode volume V reads

$$\hat{\boldsymbol{E}}(\hat{\boldsymbol{R}}) = \mathrm{i}\mathcal{E}_0\boldsymbol{u}(\hat{\boldsymbol{R}})\left(\hat{a} - \hat{a}^\dagger\right)\,, \tag{5.1.44}$$

where $\mathcal{E}_0 \equiv \sqrt{\hbar\Omega/(2\varepsilon_0 V)}$ denotes the vacuum electric field or the electric field per photon. With the help of (5.1.41) we find the interaction Hamiltonian

$$\hat{H}_{\boldsymbol{r}\cdot\boldsymbol{E}} = \hbar\left(\hat{g}\hat{\sigma}^\dagger - \hat{g}^\dagger\hat{\sigma}\right)\left(\hat{a} - \hat{a}^\dagger\right) = \hbar\left(\hat{g}\hat{\sigma}^\dagger\hat{a} - \hat{g}\hat{\sigma}^\dagger\hat{a}^\dagger - \hat{g}^\dagger\hat{\sigma}\hat{a} + \hat{g}^\dagger\hat{\sigma}\hat{a}^\dagger\right)\,, \tag{5.1.45}$$

where the operator $\hat{g}$ is given by $\hat{g}(\hat{\boldsymbol{R}}) = -\mathrm{i}\mathcal{E}_0(\boldsymbol{\wp}\cdot\boldsymbol{u}(\hat{\boldsymbol{R}}))/\hbar$. This Hamiltonian contains operator products $\hat{\sigma}\hat{a}$ and $\hat{\sigma}^\dagger\hat{a}^\dagger$. They correspond to the annihilation of a photon together with a transition from the excited to the ground state and the creation of a photon together with the excitation of an atom. When we solve the Schrödinger equation perturbatively these operator products lead to higher-order contributions. Neglecting them amounts to the rotating-wave approximation.

In the rotating-wave approximation this simple model for the position-dependent interaction of a two-level atom with a single mode of the radiation field with frequency Ω is summarized by the Hamiltonian

$$\hat{H} = \frac{\hat{\boldsymbol{P}}^2}{2M} + \hbar\Omega\,\hat{a}^\dagger\hat{a} + \frac{1}{2}\hbar\omega\hat{\sigma}_z + \hbar\left(\hat{g}\hat{\sigma}^\dagger\hat{a} + \hat{g}^\dagger\hat{\sigma}\hat{a}^\dagger\right)\,. \tag{5.1.46}$$

5.1.4.2.2 Dynamics of Jaynes–Cummings–Paul model

We can simplify the model even further when we keep the position of the atom fixed, that is we neglect the kinetic energy and replace the operator $\hat{\boldsymbol{R}}$ by a fixed vector $\boldsymbol{R}_0$. In this case, the Jaynes–Cummings–Paul model [63Jay, 63Pau] with the Hamiltonian

$$\hat{H}_{\mathrm{JCP}} \equiv \hbar\Omega\,\hat{a}^\dagger\hat{a} + \frac{1}{2}\hbar\omega\hat{\sigma}_z + \hbar g\left(\hat{\sigma}\hat{a}^\dagger + \hat{\sigma}^\dagger\hat{a}\right) \tag{5.1.47}$$

can be solved exactly. Here we have chosen the phases of the states $|\,a\,\rangle$ and $|\,b\,\rangle$ such that $\boldsymbol{\wp}\cdot\boldsymbol{u}(\boldsymbol{R}_0)$ is purely imaginary which allows us to introduce the vacuum Rabi frequency $g \equiv |\boldsymbol{\wp}\cdot\boldsymbol{u}(\boldsymbol{R}_0)|\,\mathcal{E}_0/\hbar$. For a detailed review of this model we recommend [90Sho, 93Sho].

Due to the particular atom–field coupling $\hat{\sigma}\hat{a}^\dagger$ and $\hat{\sigma}^\dagger\hat{a}$ the time-dependent solution of the Schrödinger equation is of the form

$$|\,\Psi(t)\,\rangle = \sum_{n=0}^{\infty}\left[\Psi_{a,n}(t)|\,a,n\,\rangle + \Psi_{b,n+1}(t)|\,b,n+1\,\rangle\right] + \Psi_{b,0}(t)|\,b,0\,\rangle\,, \tag{5.1.48}$$

where we have defined the states $|\,a,n\,\rangle \equiv |\,a\,\rangle|\,n\,\rangle$ and $|\,b,n\,\rangle \equiv |\,b\,\rangle|\,n\,\rangle$. In the interaction picture defined by $\hat{H}_0 = \hbar\Omega\,\hat{a}^\dagger\hat{a} + \frac{1}{2}\hbar\omega\hat{\sigma}_z$ the probability amplitudes

$$\begin{aligned}
&\Psi_{a,n}(t) = \mathrm{e}^{-\mathrm{i}\Delta t/2}\left\{\left[\cos(\lambda_n t) + \mathrm{i}\delta_n \sin(\lambda_n t)\right]\Psi_{a,n}(0) - \mathrm{i}\varepsilon_n \sin(\lambda_n t)\Psi_{b,n+1}(0)\right\}\ ,\\
&\Psi_{b,n+1}(t) = \mathrm{e}^{\mathrm{i}\Delta t/2}\left\{-\mathrm{i}\varepsilon_n \sin(\lambda_n t)\Psi_{a,n}(0) + \left[\cos(\lambda_n t) - \mathrm{i}\delta_n \sin(\lambda_n t)\right]\Psi_{b,n+1}(0)\right\}\ ,\\
&\Psi_{b,0}(t) = \Psi_{b,0}(0)
\end{aligned} \tag{5.1.49}$$

contain the detuning $\Delta \equiv \Omega - \omega$ between the field and the atomic transition frequencies and the generalized Rabi frequencies $\lambda_n \equiv \sqrt{g^2(n+1) + (\Delta/2)^2}$. Moreover, we have introduced the abbreviations $\delta_n \equiv \Delta/(2\lambda_n)$ and $\varepsilon_n \equiv g\sqrt{n+1}/\lambda_n$.

5.1.4.2.3 Quantum motion in an ion trap

The Hamiltonian, (5.1.47), of the Jaynes–Cummings–Paul model can also be used to describe [92Blo, 94Cir] the center-of-mass motion of a two-level ion trapped in a harmonic potential and interacting with an appropriate classical field. In this application the operators $\hat{a}$ and $\hat{a}^\dagger$ are the annihilation and creation operators of the mechanical harmonic oscillator representing the center-of-mass motion of the ion in the trap. The coupling between the internal degrees of freedom and the motion is achieved by a classical electromagnetic field characterized by a coupling constant g. Even an anti-Jaynes–Cummings–Paul model [97Buz] and a nonlinear Jaynes–Cummings–Paul model [95Vog] can be formulated for this mechanical analog. Moreover, a whole gallery of non-classical states of motion has been realized experimentally [96Mee].

We conclude by noting that a Paul trap [90Pau] is a time-dependent harmonic oscillator. Nevertheless, the time-dependent nonlinear Jaynes–Cummings–Paul model allows for analytical solutions [96Bar, 97Sch].

5.1.4.3 Quantum state engineering

In the preceding section we have presented the exact solution of the Jaynes–Cummings–Paul model for arbitrary detuning. In the present section we briefly discuss the two extreme cases of $\Delta = 0$ and Δ very large. Both cases allow us to prepare special field states.

5.1.4.3.1 Resonant case: photon number state preparation

We start our discussion with the preparation of a Fock state $|\,N\,\rangle$ of N photons in a cavity. We assume that the resonator is initially in the vacuum state $|\,0\,\rangle$ and we inject N excited atoms one by one. Here we assume for the sake of simplicity that there is only one single atom in the cavity at a time. In this case, the interaction of each atom with the cavity field is governed by the Jaynes–Cummings–Paul model. For $\Delta = 0$ the time-dependent solution, (5.1.49), shows that for an appropriate interaction time an excited atom can deposit its excitation into the cavity field with unit probability. Since the Rabi frequency depends on the number of photons, the interaction time of every atom has to be different. Provided all N atoms transfer their excitation to the field we have, indeed, engineered the Fock state $|\,N\,\rangle$.

Such an experiment has been performed [00Var] using the microwave resonator of the one-atom maser in Garching. Starting from the vacuum state the experimentalists have created successively a one-photon and a two-photon state. They have probed these states with an additional atom and have measured the Rabi oscillations of this atom due to the so-prepared field as shown in Fig. 5.1.3.

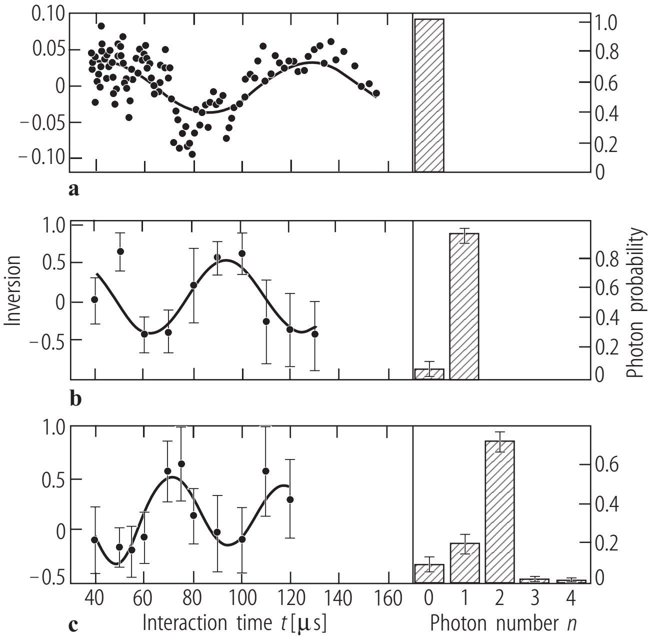

Fig. 5.1.3. Fock state preparation and measurement. A sequence of two-level atoms passing an initially empty high-Q cavity (**a**) can prepare and probe a one-photon (**b**) or a two-photon Fock state (**c**) by giving the atomic excitation into the field and by measuring the resulting Rabi oscillations. Taken from [00Var].

5.1.4.3.2 Far off-resonant case: Schrödinger cat state preparation

Another interesting limit of the Jaynes–Cummings–Paul model arises for large detuning, that is for $|\Delta| \gg g\sqrt{n+1}$. Within this approximation the dynamics of the Jaynes–Cummings–Paul model can be described by the effective Hamiltonian [01Sch]

$$\hat{H}_{\text{eff}} \equiv -\frac{\hbar g^2}{\Delta}\left[\hat{\sigma}_z\,\hat{n} + \frac{1}{2}\left(\hat{\sigma}_z + \mathbb{1}\right)\right] . \tag{5.1.50}$$

Since the Hamiltonian only contains $\hat{\sigma}_z$ as well as the photon number operator $\hat{n}$ it does not cause any transitions in the system. It conserves the populations in the atomic levels and the photon number. However, it introduces phase shifts in the field which depend on the state of the atom.

We make use of this fact [96Bru] to prepare the Schrödinger cat state, (5.1.31). For this purpose we add classical light fields at the entrance and the exit of the resonator. The first field prepares the atom in a coherent superposition of its internal states and the second field measures the so-prepared dipole. In this Ramsey setup both fields have a fixed phase relation with each other. The quantized field in the resonator is initially in a coherent state $|\,\alpha\,\rangle$.

The photon number states accumulate phases whose sign depend on the internal states of the atom. The first field can be chosen such that the state of the combined system reads

$$|\,\Psi\,\rangle = \frac{1}{\sqrt{2}}\left[|\,\alpha e^{i\varphi}\,\rangle|\,a\,\rangle + |\,\alpha e^{-i\varphi}\,\rangle|\,b\,\rangle\right] , \tag{5.1.51}$$

where the phase φ is given by $\varphi = gt^2/\Delta$.

When we now measure the atom in an atomic superposition state $|\,\psi_{\text{at}}\,\rangle \equiv \psi_a|\,a\,\rangle + \psi_b|\,b\,\rangle$ the field state reads

$$|\,\psi_{\text{cat}}\,\rangle \equiv \mathcal{N}\,\langle\psi_{\text{at}}|\,\Psi\,\rangle = \frac{\mathcal{N}}{\sqrt{2}}\left[\psi_a^*|\,\alpha e^{i\varphi}\,\rangle + \psi_b^*|\,\alpha e^{-i\varphi}\,\rangle\right] , \tag{5.1.52}$$

where $\mathcal{N}$ is the normalization factor.

In this way the Schrödinger cat state, (5.1.31), of the radiation field has been prepared experimentally [96Bru]. A similar Schrödinger cat state for the vibratory motion of a harmonically trapped ion has also been generated [00Mya].

5.1.5 Reservoir theory

So far we have concentrated on pure states of the radiation field that interact in a unitary way with atoms. However, unitary time evolution cannot describe damping or amplification. For example, the state of an electromagnetic field in a leaky cavity cannot be a pure state. We have to resort to a density operator description [01Sch].

5.1.5.1 Master equation

Several models [96Scu] provide a quantum-mechanical description of a damped radiation field. The most intuitive approach is based on a cavity field interacting with an environment modeled by a stream of resonant two-level atoms. These atoms can carry energy away from the resonator. Since the disturbance caused by them is assumed to be small we need many atoms to create a significant change of the field state. It is therefore impossible to keep track of the internal states of every atom exiting the cavity. Moreover, we are only interested in the dynamics of the field. Consequently, we trace over the atomic states and arrive at an equation of motion for the density operator of the field. It is the trace operation that introduces irreversibility into this model.

5.1.5.1.1 Mathematics of the model

When we describe the interaction by the Jaynes–Cummings–Paul Hamiltonian the state of the complete system of atom and field is determined by (5.1.48). In this solution we take the trace over the atomic variables. As a result we find the density operator $\hat{\rho}_{\mathrm{f}}(t+\tau)$ of the field after the interaction time τ.

So far, we have only considered the dynamics of the field due to the interaction with a single atom. We now take into account the influence of a stream of atoms injected into the cavity with a rate r. Since each individual atom only introduces a small change we can approximate the dynamics of the field by the coarse-grained master equation

$$\frac{\mathrm{d}}{\mathrm{d}t}\hat{\rho}_{\mathrm{f}}(t) \approx r\left[\hat{\rho}_{\mathrm{f}}(t+\tau) - \hat{\rho}_{\mathrm{f}}(t)\right] . \tag{5.1.53}$$

Moreover, it is sufficient to retain terms quadratic in $g\tau$. The resulting equation of motion reads

$$\begin{aligned}\frac{\mathrm{d}}{\mathrm{d}t}\,\hat{\rho}_{\mathrm{f}}(t) = \mathcal{L}(\hat{\rho}_{\mathrm{f}}) \equiv -\frac{1}{2}\,\mathcal{R}_a\left[\hat{a}\,\hat{a}^\dagger\,\hat{\rho}_{\mathrm{f}}(t) + \hat{\rho}_{\mathrm{f}}(t)\,\hat{a}\,\hat{a}^\dagger - 2\hat{a}^\dagger\,\hat{\rho}_{\mathrm{f}}(t)\,\hat{a}\right]\\ -\frac{1}{2}\,\mathcal{R}_b\left[\hat{a}^\dagger\,\hat{a}\,\hat{\rho}_{\mathrm{f}}(t) + \hat{\rho}_{\mathrm{f}}(t)\,\hat{a}^\dagger\,\hat{a} - 2\hat{a}\,\hat{\rho}_{\mathrm{f}}(t)\,\hat{a}^\dagger\right] .\end{aligned} \tag{5.1.54}$$

Here we have introduced the abbreviations $\mathcal{R}_a \equiv r\,\rho_{aa}\,(g\tau)^2$ and $\mathcal{R}_b \equiv r\,\rho_{bb}\,(g\tau)^2$, where ρ_{aa} and ρ_{bb} denote the populations in the two levels of the atoms. Furthermore, we have assumed a vanishing polarization $\rho_{ab} = 0$.

5.1.5.1.2 Methods of solution

Equations for the density operator of a subsystem such as (5.1.54) carry the name master equations. They are operator equations and usually involve a Liouville operator $\mathcal{L}$ acting on the density operator. In the present case the Liouville operator contains only operators of the field mode. Moreover, the order of the individual operators is important. For this reason it is not straightforward to solve master equations. Several methods [85Gar, 89Ris, 91Gar] offer themselves:

Matrix elements [89Coh, 91Mey, 92Coh, 94Wal, 96Scu, 01Sch]: An expansion of the density operator in terms of Fock states leads to equations of motions for the matrix elements forming a coupled system of ordinary linear differential equations.

Phase space distributions [63Gla1, 63Gla2, 63Sud, 69Cah, 84Hil]: The master equation for the density operator can be transformed into an equation of motion for a phase space distribution which is a linear partial differential equation.

Quantum jump method [93Car]: Here a stochastic sequence of jump processes and non-unitary time evolutions based on a Schrödinger equation with a non-hermitean Hamiltonian is solved numerically. By averaging over all trajectories we obtain a numerical solution of the master equation.

5.1.5.2 Damping and amplification

For the case of the master equation, (5.1.54), these techniques show the following results. When more atoms enter the cavity in the *excited state* rather than in the ground state, that is $\rho_{aa} > \rho_{bb}$ we find an *amplification* of the field. On average more atoms deposit their excitation than atoms take photons out of the cavity.

However, when more atoms enter the cavity in the *ground state* rather than in the excited state, that is $\rho_{bb} > \rho_{aa}$ we find a *damping* of the field. On average more atoms withdraw excitations than atoms deposit photons into the cavity. Independent of the initial state the cavity field eventually approaches a thermal state, (5.1.38), with a temperature T determined by the initial atomic populations. The average number of thermal photons $n_{\text{th}} = [\exp[\hbar\omega/(k_{\text{B}}T)] - 1]^{-1} = [\rho_{bb}/\rho_{aa} - 1]^{-1}$ in the limit of $t \to \infty$ and the decay rate $\kappa \equiv \mathcal{R}_b - \mathcal{R}_a = r(g\tau)^2(\rho_{bb} - \rho_{aa})$ allow us to cast the Liouville operator $\mathcal{L}_{\text{damp}}$ of damping into the form

$$\mathcal{L}_{\text{damp}}(\hat{\rho}_{\text{f}}) \equiv -\frac{\kappa}{2}(n_{\text{th}}+1)\left(\hat{a}^\dagger\hat{a}\hat{\rho}_{\text{f}} + \hat{\rho}_{\text{f}}\hat{a}^\dagger\hat{a} - 2\hat{a}\hat{\rho}_{\text{f}}\hat{a}^\dagger\right) - \frac{\kappa}{2}n_{\text{th}}\left(\hat{a}\hat{a}^\dagger\hat{\rho}_{\text{f}} + \hat{\rho}_{\text{f}}\hat{a}\hat{a}^\dagger - 2\hat{a}^\dagger\hat{\rho}_{\text{f}}\hat{a}\right) . \quad (5.1.55)$$

We emphasize that $\mathcal{L}_{\text{damp}}$ only contains field quantities such as the cavity decay constant κ and the average number n_{th} of photons together with field operators.

5.1.5.3 Decoherence

The superposition principle is one of the corner stones of quantum mechanics. Indeed, as P.A.M. Dirac states in his famous textbook [35Dir] "... any two or more states may be superposed to give a new state". The example of the Schrödinger cat state, (5.1.31), demonstrates the power of this principle. Both coherent states forming the cat are classical states. However, their superposition is a highly non-classical state [91Sch].

The non-classical features arising from the superposition principle stand out most clearly in $|\,\psi_{\text{cat}}\,\rangle$ for two coherent states of large amplitude α and a large angle 2φ between them, see Fig. 5.1.1. For this set of parameters we can distinguish the two individual states but still observe the interference between them. Since our classical world does not contain such superpositions of distinguishable states the question arises: What is the mechanism that erases the interference terms [91Zur, 96Giu] when we cross the border from the quantum to the classical world?

Niels Bohr has always insisted that a measurement apparatus has to be described in classical terms involving "irreversible amplification" [58Boh]. Irreversibility implies many degrees of freedom. It is the feature of the many degrees of freedom that erases the quantum interference.

We now illustrate this concept using the example of the measurement of a cavity field. For this purpose we extract a portion of the field from the resonator, that is we couple it to the modes of the measurement apparatus. Therefore, we arrive at the problem of a single mode coupled to

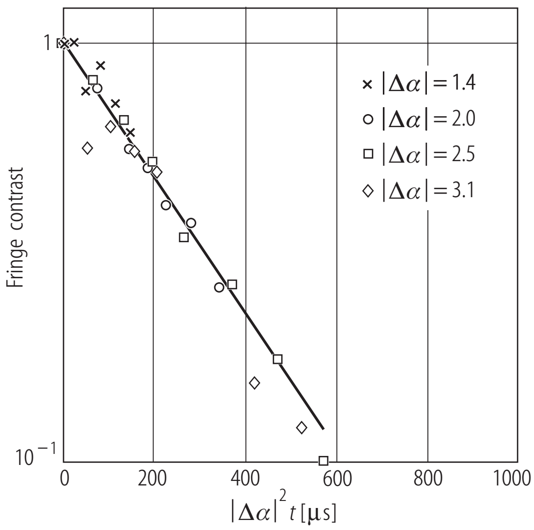

Fig. 5.1.4. Decoherence of a Schrödinger cat state coupled to a thermal reservoir, here demonstrated for the center-of-mass motion of an ion in a trap. The contrast of the interference fringes decreases as a function of time t. The decay depends on the square of the separation $|\Delta\alpha|$ of the individual constituents. The solid line is a fit to an exponential decay law. Taken from [00Mya].

many more field modes. The corresponding Liouville operator for this damping model is identical to (5.1.55). The number n_{th} of thermal photons in this case is determined by the state of the reservoir and κ is the decay constant of the cavity. Consequently, the dynamics of the cavity field in the interaction picture is determined by $\dot{\hat{\rho}}_{\text{f}} = \mathcal{L}_{\text{damp}}(\hat{\rho}_{\text{f}})$ with the Liouville operator $\mathcal{L}_{\text{damp}}$, (5.1.55).

Deeper insight into the tantalizing question of the emergence of the classical world follows from this master equation when we consider as an initial state the Schrödinger cat

$$\begin{aligned}\hat{\rho}_{\text{cat}} &\equiv |\,\psi_{\text{cat}}\,\rangle\langle\,\psi_{\text{cat}}\,| \\ &= |\mathcal{N}|^2\left[|\,\alpha e^{i\varphi}\,\rangle\langle\,\alpha e^{i\varphi}\,| + |\,\alpha e^{-i\varphi}\,\rangle\langle\,\alpha e^{-i\varphi}\,| + |\,\alpha e^{i\varphi}\,\rangle\langle\,\alpha e^{-i\varphi}\,| + |\,\alpha e^{-i\varphi}\,\rangle\langle\,\alpha e^{i\varphi}\,|\right]\end{aligned} \tag{5.1.56}$$

shown in Fig. 5.1.1.

Indeed, a treatment using any of the three methods outlined in Sect. 5.1.5.1.2 shows that the diagonal elements $|\,\alpha e^{i\varphi}\,\rangle\langle\,\alpha e^{i\varphi}\,|$ and $|\,\alpha e^{-i\varphi}\,\rangle\langle\,\alpha e^{-i\varphi}\,|$ decay with the decay constant κ of the cavity. However, the off-diagonal terms $|\,\alpha e^{i\varphi}\,\rangle\langle\,\alpha e^{-i\varphi}\,|$ and $|\,\alpha e^{-i\varphi}\,\rangle\langle\,\alpha e^{i\varphi}\,|$, that is the interference terms, decay much faster. The decay constant of these contributions is determined by the product $\kappa\,(2\alpha\sin\varphi)^2$ of the decay rate of the cavity and the square of the separation $\Delta\alpha = 2\alpha\sin\varphi$ of the coherent states in phase space shown in Fig. 5.1.1. Hence, when they are far apart and we can easily distinguish them, the interferences decay on a much faster time scale and we are left with a mixed state $\hat{\rho} = \left(|\,\alpha e^{i\varphi}\,\rangle\langle\,\alpha e^{i\varphi}\,| + |\,\alpha e^{-i\varphi}\,\rangle\langle\,\alpha e^{-i\varphi}\,|\right)/2$ which only contains diagonal elements.

This mechanism of decoherence arises when we couple a system to a reservoir. It eliminates quantum-mechanical interference between macroscopically distinguishable states. The enhanced decay of interference structures has been observed using Schrödinger cat states in cavity QED [96Bru] and ion experiments [00Mya]. In particular, the quadratic dependence on the separation of the two contributing states has been verified as shown in Fig. 5.1.4.

5.1.6 One-atom maser

The combination of superconducting cavities with Rydberg atoms has created a new light source with highly unusual quantum-statistical properties. In this amazing maser [94Rai] a weak beam of excited two-level atoms traverses a cavity with a quality factor of 10^{10} and interacts resonantly with a single mode of the radiation field. The flux of the atomic beam is so small that at most one atom at a time is in the cavity. The atom can deposit its excitation in the cavity and in this way amplify the field. The atom also serves a different purpose: It probes the field. A detector after the resonator measures the population of the internal levels.

5.1.6.1 Master equation

We describe this interaction by the resonant Jaynes–Cummings–Paul (JCP) Hamiltonian in the interaction picture. By taking the trace over the atomic degrees of freedom we find [01Sch] the coarse-grained equation of motion

$$\frac{\mathrm{d}}{\mathrm{d}t}\,\hat{\rho}_{\mathrm{f}}(t) \equiv \mathcal{L}_{\mathrm{JCP}}(\hat{\rho}_{\mathrm{f}}) \equiv r[\hat{C}_n(\tau)\,\hat{\rho}_{\mathrm{f}}(t)\,\hat{C}_n(\tau) - \hat{\rho}_{\mathrm{f}}(t)] + r\,\frac{\hat{S}_{n-1}(\tau)}{\sqrt{\hat{n}}}\,\hat{a}^{\dagger}\hat{\rho}_{\mathrm{f}}(t)\,\hat{a}\,\frac{\hat{S}_{n-1}(\tau)}{\sqrt{\hat{n}}}\,, \tag{5.1.57}$$

where we have introduced the abbreviations $\hat{C}_n(\tau) \equiv \cos(g\tau\sqrt{\hat{n}+1})$, $\hat{S}_n(\tau) \equiv \sin(g\tau\sqrt{\hat{n}+1})$ and the atomic injection rate r. Moreover, we have assumed that the atoms enter the cavity in the excited state, that is $\rho_{aa} = 1$ and $\rho_{bb} = \rho_{ab} = \rho_{ba} = 0$.

We assume, that the time interval between two successive atoms is much larger than the interaction time of a single atom. In this time interval we take into account the damping of the field mode by the Liouville operator $\mathcal{L}_{\mathrm{damp}}(\hat{\rho}_{\mathrm{f}})$, defined in (5.1.55). Hence the complete dynamics

$$\frac{\mathrm{d}}{\mathrm{d}t}\,\hat{\rho}_{\mathrm{f}}(t) \equiv \mathcal{L}_{\mathrm{JCP}}(\hat{\rho}_{\mathrm{f}}) + \mathcal{L}_{\mathrm{damp}}(\hat{\rho}_{\mathrm{f}}) \tag{5.1.58}$$

of the one-atom maser [86Fil, 87Lug] is governed by the sum of the two Liouville operators $\mathcal{L}_{\mathrm{JCP}}$ and $\mathcal{L}_{\mathrm{damp}}$. We emphasize that this equation of motion is an approximation which makes assumptions on the statistics of the injected atoms. Modifications of (5.1.58) due to different pump statistics are discussed in [94Ber].

5.1.6.2 Steady-state photon statistics

We first analyze the properties of the steady-state photon statistics [86Fil, 87Lug]

$$W_n \equiv \langle\, n\,|\hat{\rho}_{\mathrm{f}}|\, n\,\rangle = W_0 \prod_{l=1}^{n} \left[\frac{n_{\mathrm{th}}}{n_{\mathrm{th}}+1} + \frac{r\sin^2(g\tau\sqrt{l}\,)}{\kappa(n_{\mathrm{th}}+1)l}\right] \tag{5.1.59}$$

determined by the diagonal elements of the density operator of the one-atom maser. Here W_0 is a normalization constant.

In Fig. 5.1.5 we show the mean photon number $\langle\hat{n}\rangle$ and the normalized variance σ defined in (5.1.39) in steady state using the stationary photon statistics, (5.1.59), as a function of the dimensionless interaction time $\theta \equiv \sqrt{r/\kappa}\,g\tau$. We recognize a steep increase of $\langle\hat{n}\rangle$ as θ approaches unity which is the maser threshold. A similar effect occurs in every laser. However, due to the presence of the sine function in (5.1.59) more thresholds appear, but they are not as pronounced as the first one.

Moreover, the normalized variance σ shown in Fig. 5.1.5 by a solid curve shows that the maser oscillates between sub-Poissonian and super-Poissonian statistics. These different domains have been observed [90Rem] in experiments.

The photon statistics of the one-atom maser becomes particularly interesting when there are no thermal photons present, that is for $n_{\mathrm{th}} = 0$ or $T = 0$. When we now choose the interaction time τ such that

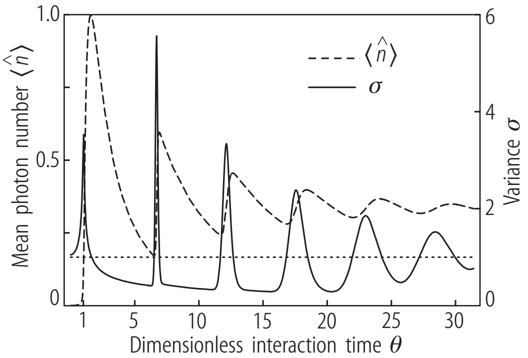

Fig. 5.1.5. Normalized mean photon number $\langle\hat{n}\rangle$ and normalized variance σ of the photon statistics of the one-atom maser in steady state as a function of the dimensionless interaction time $\theta \equiv \sqrt{r/\kappa}\, g\tau$. The pump parameter is $r/\kappa = 200$ and the dotted line indicates the value $\sigma = 1$ corresponding to a coherent state with Poissonian statistics.

$$g\tau\sqrt{n_q+1} = q\pi\,, \tag{5.1.60}$$

where q and n_q are positive integers, the steady-state photon statistics, (5.1.59), vanishes starting from the photon number n_q+1. This phenomenon carries the name "trapping state" [88Mey].

An intuitive explanation of trapping states recognizes that an excited atom interacting with the state $|\,n_q\,\rangle$ cannot deposit its excitation in the cavity because for this particular interaction time the atom undergoes an integer number of Rabi cycles and therefore leaves the cavity in the excited state. Trapping states have been observed experimentally [99Wei] in the one-atom maser.

5.1.7 Atom–reservoir interaction

Our previous studies have focused on the dynamics of a single mode driven by a reservoir of two-level atoms. In the present section we consider the dynamics of a single two-level atom under the influence of infinitely many field modes forming the reservoir. This coupling of the atom to the field reservoir leads to spontaneous emission of the atoms as well as level shifts. We briefly discuss the equation of motion for the density operator $\hat{\rho}_{\rm at}$ of the atom and analyze the consequences.

5.1.7.1 Master equation

In order to describe the atom–reservoir interaction we consider the Hamiltonian

$$\hat{H}_{\rm ar} \equiv \hat{H}_{\rm at} + \hat{H}_{\rm f} + \hat{H}_{\rm int} \equiv \frac{1}{2}\,\hbar\omega\hat{\sigma}_z + \sum_\ell \hbar\Omega_\ell \hat{a}_\ell^\dagger \hat{a}_\ell + \sum_\ell \hbar g_\ell (\hat{\sigma}\hat{a}_\ell^\dagger + \hat{\sigma}^\dagger \hat{a}_\ell)\,, \tag{5.1.61}$$

where Ω_ℓ is the frequency of the ℓth mode and $g_\ell \equiv g_\ell(\boldsymbol{R})$ denotes the coupling strength of the atom at the position $\boldsymbol{R}$ to the ℓth mode.

The resulting master equation in the interaction picture for the atomic density operator $\hat{\rho}_{\rm at}$ reads [73Lou, 01Sch]

$$\begin{aligned}\frac{\rm d}{{\rm d}t}\hat{\rho}_{\rm at} = &-\frac{\rm i}{\hbar}\left[\Delta\hat{H}, \hat{\rho}_{\rm at}\right]\\ &-(\Gamma_{\rm r}+G_{\rm r})\left[\hat{\sigma}^\dagger\hat{\sigma}\hat{\rho}_{\rm at} + \hat{\rho}_{\rm at}\hat{\sigma}^\dagger\hat{\sigma} - 2\hat{\sigma}\hat{\rho}_{\rm at}\hat{\sigma}^\dagger\right] - \Gamma_{\rm r}\left[\hat{\sigma}\hat{\sigma}^\dagger\hat{\rho}_{\rm at} + \hat{\rho}_{\rm at}\hat{\sigma}\hat{\sigma}^\dagger - 2\hat{\sigma}^\dagger\hat{\rho}_{\rm at}\hat{\sigma}\right]\\ &+2\beta^*\hat{\sigma}\hat{\rho}_{\rm at}\hat{\sigma} + 2\beta\hat{\sigma}^\dagger\hat{\rho}_{\rm at}\hat{\sigma}^\dagger\,,\end{aligned} \tag{5.1.62}$$

where we have introduced the Hamiltonian

$$\Delta \hat{H} \equiv -\hbar \left(\Gamma_{\mathrm{i}} + \frac{1}{2} G_{\mathrm{i}} \right) \hat{\sigma}_z \,. \tag{5.1.63}$$

The explicit expressions [01Sch] for the complex-valued quantities $\Gamma \equiv \Gamma_{\mathrm{r}} + \mathrm{i}\,\Gamma_{\mathrm{i}}$, $G \equiv G_{\mathrm{r}} + \mathrm{i}\,G_{\mathrm{i}}$ and $\beta \equiv \beta_{\mathrm{r}} + \mathrm{i}\,\beta_{\mathrm{i}}$ are rather complicated and can be even infinite [73Lou]. They are determined by the state of the reservoir through the expectation values of the reservoir field modes. For example, Γ depends on the average number $\langle \hat{n}_\ell \rangle$ of photons in the individual reservoir modes as well as the expectation values $\langle \hat{a}_\ell^\dagger \rangle$ and $\langle \hat{a}_\ell \rangle$. Since for a thermal reservoir we have $\langle \hat{a}_\ell \rangle = \langle \hat{a}_\ell^\dagger \rangle = 0$ it is only $\langle \hat{n}_\ell \rangle$ that determines Γ. The parameter β depends on $\langle \hat{a}_\ell^2 \rangle$ and $\langle \hat{a}_\ell \rangle$. For a thermal state both quantities vanish. However, for a squeezed vacuum we find $\langle \hat{a}_\ell^2 \rangle \neq 0$ which leads to a non-vanishing value of β. This fact has important consequences for the decay of the atomic excitation into a squeezed vacuum as discussed in [86Gar].

However, the most interesting coefficient is G since it does not contain any expectation values of the reservoir. Its origin can be traced back [01Sch] to the commutation relation between $\hat{a}_\ell$ and $\hat{a}_\ell^\dagger$. It is therefore a consequence of the quantization of the radiation field.

5.1.7.2 Lamb shift

We now turn to the correction $\Delta \hat{H}$ to the Hamiltonian $\hat{H}_{\mathrm{at}} = \frac{1}{2}\hbar\omega\hat{\sigma}_z$ of the free atom. The interaction of the atom with a reservoir of field modes leads to a level shift of frequency

$$\Delta\omega \equiv -2 \left(\Gamma_{\mathrm{i}} + \frac{1}{2}\, G_{\mathrm{i}} \right) \tag{5.1.64}$$

which carries the name Lamb shift. It has been discovered experimentally in 1947 by Willis E. Lamb and his graduate student Robert C. Retherford in hydrogen [47Lam]. The Dirac equation predicts that the $2\mathrm{S}_{1/2}$ and $2\mathrm{P}_{1/2}$ energy levels are degenerated. However, the experiment showed clearly that this degeneracy is lifted. The Lamb shift is a manifestation of the quantization of the electromagnetic field [01Sch]. Indeed, we recognize from (5.1.64) that there are two shifts: The first arises from the imaginary part Γ_{i} of Γ. Since the parameter Γ is essentially determined by the average number of photons in the reservoir modes this contribution to the level shift is analogous to the familiar second-order Stark-effect of an atom in a static electric field.

In contrast, the contribution G_{i} arises from the commutation relations of the field operators. It is therefore a pure quantum effect of the field and is nonzero even when all modes of the reservoir are in the ground state, that is in the vacuum.

5.1.7.3 Weisskopf–Wigner decay

Apart from the shift of the levels the reservoir has another dramatic effect: It forces the atom to decay, that is the populations $\rho_{aa} \equiv \langle\, a\,|\hat{\rho}_{\mathrm{at}}|\, a\,\rangle$ and $\rho_{bb} \equiv \langle\, b\,|\hat{\rho}_{\mathrm{at}}|\, b\,\rangle$ in the two levels and the polarization $\rho_{ab} \equiv \langle\, a\,|\hat{\rho}_{\mathrm{at}}|\, b\,\rangle$ change as a function of time. This phenomenon carries the name Weisskopf–Wigner decay.

We now consider all reservoir modes being in the vacuum state. In this case the coefficients Γ and β vanish. When we introduce the decay constant $\gamma \equiv 2G_{\mathrm{r}}$ of the atom, (5.1.62) reduces to the master equation

$$\frac{\mathrm{d}}{\mathrm{d}t}\hat{\rho}_{\mathrm{at}} = \mathcal{L}_{\mathrm{sp}}(\hat{\rho}_{\mathrm{at}}) \equiv -\frac{1}{2}\gamma \left[\hat{\sigma}^\dagger \hat{\sigma} \hat{\rho}_{\mathrm{at}} + \hat{\rho}_{\mathrm{at}} \hat{\sigma}^\dagger \hat{\sigma} - 2\hat{\sigma}\hat{\rho}_{\mathrm{at}}\hat{\sigma}^\dagger \right] \tag{5.1.65}$$

of spontaneous emission, where we have omitted the Lamb shift term $\left[\Delta\hat{H}, \hat{\rho}_{\mathrm{at}}\right]$.

When we now take matrix elements of the atomic density operator in the energy basis, that is project from left and right with energy states $|\,a\,\rangle$ and $|\,b\,\rangle$ on (5.1.65), we arrive at the equations of motion

$$\dot{\rho}_{aa} = -\gamma\rho_{aa}, \quad \dot{\rho}_{bb} = +\gamma\rho_{aa}\,, \quad \dot{\rho}_{ab} = -\frac{\gamma}{2}\rho_{ab}\,. \tag{5.1.66}$$

Hence the population of the excited state decays, but due to the conservation $\rho_{aa} + \rho_{bb} = 1$ of probability, the population in the ground state grows. Moreover, the polarization ρ_{ab} also decays and the atom finally ends up in its ground state.

5.1.8 Resonance fluorescence

We now consider a two-level atom driven by a classical monochromatic wave. The excited state of the atom can decay by spontaneous emission into vacuum modes of the electromagnetic field. This emission is called resonance fluorescence. Of particular interest are the quantum-statistical properties of the emitted light. For a detailed discussion of resonance fluorescence, see for example [91Mey, 92Coh, 93Car, 94Wal].

5.1.8.1 Model

The electromagnetic field radiated by an atom located at the origin is in the far field proportional to its dipole moment and can therefore be expressed in terms of the Pauli operators $\hat{\sigma}$ and $\hat{\sigma}^\dagger$ [93Car]. Knowledge of $\hat{\sigma}$ and $\hat{\sigma}^\dagger$ is therefore sufficient to study the properties of the emitted light in the far field. We therefore consider a two-level atom driven by a classical field and coupled to the reservoir discussed in Sect. 5.1.7.

The total Hamiltonian for this model system describing resonance fluorescence then reads

$$\hat{H}_{\mathrm{rf}} \equiv \hat{H}_{\mathrm{ar}} + \frac{1}{2}\hbar\Omega_{\mathrm{R}}\left(\hat{\sigma}\mathrm{e}^{\mathrm{i}\omega t} + \hat{\sigma}^\dagger\mathrm{e}^{-\mathrm{i}\omega t}\right)\,, \tag{5.1.67}$$

where we have added a resonant driving term to the Hamiltonian $\hat{H}_{\mathrm{ar}}$, (5.1.61), of the atom–reservoir interaction and Ω_{R} is the Rabi frequency associated with the driving field.

The corresponding master equation in the interaction picture takes the form

$$\frac{\mathrm{d}}{\mathrm{d}t}\,\hat{\rho}_{\mathrm{at}} = -\,\frac{\mathrm{i}}{2}\,\Omega_{\mathrm{R}}\,\left[\hat{\sigma} + \hat{\sigma}^\dagger, \hat{\rho}_{\mathrm{at}}\right] + \mathcal{L}_{\mathrm{sp}}(\hat{\rho}_{\mathrm{at}})\,, \tag{5.1.68}$$

where the modes of the thermal reservoir are in the vacuum as described by (5.1.65).

5.1.8.2 Spectrum and antibunching

One of the quantities of interest is the spectrum of the emitted radiation. According to the Wiener–Khintchine theorem [95Man] this spectrum is determined by the autocorrelation function of the electric field. As mentioned the electric field follows from the dipole. As a consequence we need to

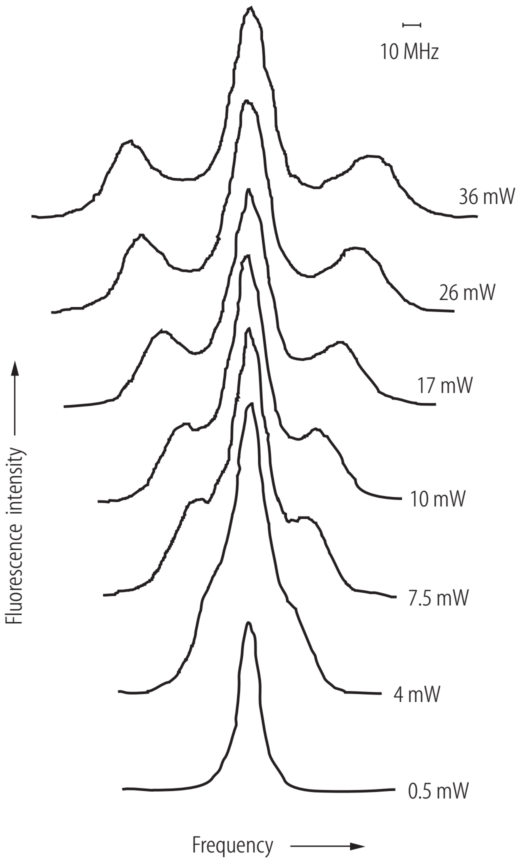

Fig. 5.1.6. Experimental three-peak Mollow spectrum for increasing laser intensity. We note the emergence of the side peaks. The elastic peak ideally represented by a delta function located on top of the central peak is not shown. Taken from [76Har].

calculate the autocorrelation function of the dipole [91Mey, 93Car]. For this purpose we take matrix elements of the master equation, (5.1.68), in the energy representation. The resulting equations are the Bloch equations.

The autocorrelation function is the expectation value of the product of the operators $\hat{\sigma}^\dagger(t)$ and $\hat{\sigma}(0)$ at two different times t and $t = 0$. In order to calculate such expectation values we make use of the quantum regression theorem which allows us to reduce two-time correlation functions to one-time expectation values. For more details we refer to [96Scu].

The result of this calculation shows that the steady-state spectrum of the fluorescence light consists of two contributions: a coherent part $S_{\mathrm{coh}}(\nu)$ and an incoherent part $S_{\mathrm{inc}}(\nu)$. The coherent part

$$S_{\mathrm{coh}}(\nu) \propto \frac{\Omega_{\mathrm{R}}^2 \gamma^2}{\left(\gamma^2 + 2\Omega_{\mathrm{R}}^2\right)^2}\, \delta(\nu - \omega) \tag{5.1.69}$$

contains a Dirac delta function. This is in analogy to a driven classical dipole that radiates at the frequency of the driving field.

The incoherent part of the fluorescence light displays two qualitatively different spectra depending on the value of the Rabi frequency. For $\Omega_{\mathrm{R}} < \gamma/4$ it has a single peak at the atomic transition frequency ω, whereas for $\Omega_{\mathrm{R}} > \gamma/4$ it consists of three peaks – the so-called Mollow-triplet, see Fig. 5.1.6. For $\Omega_{\mathrm{R}} \gg \gamma/4$ we can represent the spectrum

$$S_{\mathrm{inc}}(\nu) \propto \frac{1}{2\pi\gamma}\left[\mathcal{D}(\nu-\omega,\gamma/2) + \frac{1}{3}\,\mathcal{D}(\nu-\omega+\Omega_{\mathrm{R}},3\gamma/4) + \frac{1}{3}\,\mathcal{D}(\nu-\omega-\Omega_{\mathrm{R}},3\gamma/4)\right] \tag{5.1.70}$$

by the sum of three Lorentzians $\mathcal{D}(\xi, \Gamma) \equiv \Gamma^2/\left(\xi^2 + \Gamma^2\right)$ centered at the frequencies $\nu = \omega$ and $\nu = \omega \pm \Omega_R$ with different width and heights. The central peak at $\nu = \omega$ has a width of $\gamma/2$, whereas the width of the two side peaks at $\nu = \omega \pm \Omega_R$ is $3\gamma/4$. Their heights are one third of the height of the central peak. This spectrum was predicted by Anatoly I. Burshtein [65Bur] and Benjamin R. Mollow [69Mol] and experimentally confirmed in a series of experiments [74Sch, 75Wu, 76Har], as shown in Fig. 5.1.6.

Resonance fluorescence also displays another interesting effect: The photons of the emitted radiation tend to be separated. This tendency is known as photon antibunching [76Car1, 76Car2] and was experimentally verified [77Kim, 78Kim]. This phenomenon has a simple explanation: After the atom has emitted a photon it is in the ground state and must first be excited again before it can emit another photon. The use of a single ion stored in a Paul trap [98Win] or an atom in a magneto-optical trap [93Hau] have led to extremely clear verifications of photon antibunching.

We conclude by mentioning that also squeezing in the resonance fluorescence has been detected [98Lu]. Moreover, antibunching of free electrons has been observed recently [02Kie, 02Spe].

5.1.9 Fundamental questions of quantum mechanics

The interpretation of quantum mechanics has been and still is the subject of a longstanding debate. For many years this topic has been confined to purely theoretical discussions. However, the enormous progress in the experimental tools of quantum optics has now promoted such gedanken experiments to real world experiments. In the present section we highlight the experiments on quantum jumps, illustrate quantum-optical tests of complementarity and present violations of Bell's inequalities. Space does not allow us to do justice to the field of entangled photon pairs and beam splitting experiments with correlated photons. For this topic we refer to Sect. 6.1.4.5 of this volume and to the overviews [88Bre, 91Bre].

5.1.9.1 Quantum jumps

Our understanding of the internal dynamics of atoms has undergone dramatic changes: from the static raisin model of Joseph J. Thomson [1904Tho] via the Bohr–Sommerfeld planetary concept to the atom in QED [49Kro]. However, even the Heisenberg–Schrödinger quantum atom is still full of surprises.

5.1.9.1.1 Continuous versus discontinuous dynamics

Electrons in atoms do not move on circles or ellipses around the nucleus, but declare themselves in transitions from one Bohr orbit to another, that is in quantum jumps. These quantum jumps form the building blocks of Werner Heisenberg's matrix mechanics [25Hei, 30Bor]. Erwin Schrödinger's wave mechanics takes the completely opposite point of view. It describes a quantum system in terms of a wave function which undergoes a continuous change in time governed by the familiar Schrödinger equation.

These on first sight contradictory pictures occupied the founders of quantum mechanics. On a visit to Copenhagen in 1926 Niels Bohr kept discussing the issue of quantum jumps with Schrödinger to such an extent that eventually Schrödinger fell ill and had to stay in bed. Even then Bohr kept pestering him. Finally Schrödinger exclaimed "If we are going to have to put up with these damn quantum jumps, I am sorry that I ever had anything to do with quantum theory". Bohr's answer: "But the rest of us are very thankful for it . . . " [94Moo].

The ultimate resolution of this puzzle was provided by Schrödinger [26Sch1] showing that both approaches are different sides of the same coin. It is interesting to note that also Wolfgang Pauli in a letter to Pascual Jordan had arrived at the same conclusions but did not publish it since Schrödinger's paper had appeared in the meantime [79Pau]. In 1926 Jordan used the matrix mechanics to provide a quantum-mechanical theory of quantum jumps [27Jor].

5.1.9.1.2 Experimental observation

In 1952 Schrödinger returned to the question of quantum jumps in two papers [52Sch1, 52Sch2] entitled "Are there quantum jumps?". Schrödinger was wondering if quantum jumps could ever be observed in an experiment. His answer "No!" was based on the fact that at that time one could not imagine to experiment with single atoms. To quote from his paper: "... we are not *experimenting* with single particles, any more than we can raise Ichthyosauria in the zoo" [52Sch2].

Due to the invention of ion traps this impossibility argument no longer holds true. Indeed, Hans G. Dehmelt had suggested [75Deh] to demonstrate quantum jumps using a single ion stored in a Paul trap. For this purpose he investigated a three-level atom in a V-configuration with two excited levels and a common ground state. The transitions between ground and excited levels are driven by two resonant laser fields. The life times of the two upper levels are utterly different and we observe the fluorescence on the transition from the level with the fast decay.

The experimental result displayed in Fig. 5.1.7 shows the light emitted from a single ion driven in such a way. At random instances of time we find dark periods. During this time the atom has made a transition to the excited state with the slow decay.

We conclude by mentioning that many experiments [86Ber, 86Nag, 86Sau] have observed quantum jumps. Moreover, this phenomenon has important applications in the context of frequency measurements [00Zan] and the development of a quantum computer based on ions.

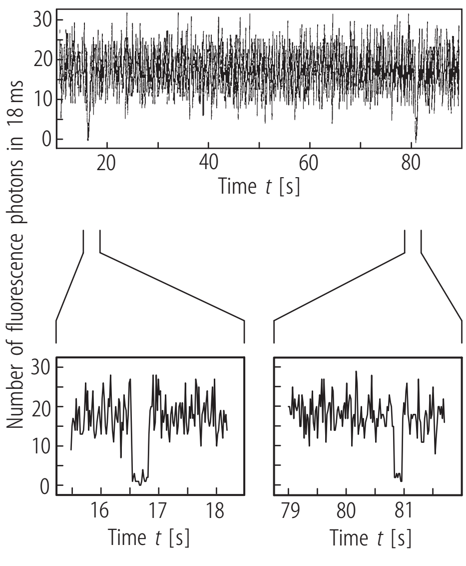

Fig. 5.1.7. Experimental observation of quantum jumps in In^+. The fluorescence light from the laser-driven transition $1S_0$–$3P_1$ is observed. From time to time the atom jumps spontaneously from the $3P_1$ level to the meta-stable $3P_0$ level. During these periods no fluorescence is observed as can be seen from the dips in the fluorescence light in the insets. Picture kindly provided by Joachim von Zanthier, Max-Planck-Institut für Quantenoptik, Garching.

5.1.9.2 Wave–particle duality

Two hundred years ago Thomas Young demonstrated the wave nature of light by his now famous double-slit experiment [1802You, 64Bor]. At the turn of the last century the question emerged if this wave nature also manifests itself in the limit of low light intensities, in particular in the limit of single photons. For this reason many experiments with attenuated light sources have been performed. However, only recently clean quantum-optics experiments could answer this question with a definitive "Yes!". For example, the experiment of [86Gra, 89Asp] feeds the antibunched light emitted by an atom into a Mach–Zehnder interferometer, shown in Fig. 5.1.8. The phenomenon of antibunching guarantees that there is only one photon at a time in the apparatus. By repeating the experiment many times the familiar interference pattern emerges.

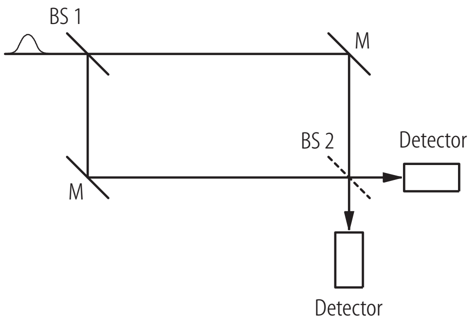

Fig. 5.1.8. Mach–Zehnder interferometer consisting of two beam splitters (BS) and two mirrors (M). We observe either interference (beam splitter BS 2 inserted) or obtain path information (beam splitter BS 2 removed). In the delayed choice mode of operation we insert BS 2 only after the photon has passed BS 1.

Young's double-slit experiment has also played a central role in the Bohr–Einstein dialog [83Whe] on wave–particle duality. This discussion centers around the question: Is it possible to construct an experimental setup that provides information about the path of the photon and at the same time displays interference? The Mach–Zehnder interferometer of Fig. 5.1.8 illustrates the point of question. Imagine a situation in which the second beam splitter is removed. A single photon entering the interferometer at the first beam splitter triggers only one of the two detectors. In this way we obtain information about the path of the photon. Detectors which provide such information carry the name "which-path" detectors, or in the German version "welcher Weg" detectors.

The fact that we have to either insert or take out the second beam splitter already indicates that we cannot obtain simultaneously in the very same experiment complete which-path *and* interference information. Niels Bohr felt that this exclusiveness of two observables is a central feature of quantum mechanics. He called [28Boh] mutual exclusive properties such as which-path and interference "complementary variables". His principle of complementarity is closely related to Heisenberg's uncertainty principle. However, the question which principle is the more fundamental is not resolved yet [96Eng].

An interesting manifestation of complementarity and wave–particle duality appears in resonance fluorescence [97Hoe]. The coherently scattered radiation displays a fixed phase relation with respect to the driving field reflecting the wave nature of light. On the other hand the same radiation exhibits photon antibunching which is a consequence of the quantum nature of light and matter. However, two different experimental setups are necessary to observe these complementary features. The first relies on a homodyne setup whereas the second one needs a correlation measurement.

5.1.9.2.1 Delayed choice experiments

A rather paradoxical situation occurs when we start from a Mach–Zehnder interferometer where initially the second beam splitter is removed. We insert it only after the photon has passed through the first beam splitter and is well on its way towards the detectors. Does this delayed choice experiment [31Wei, 41Wei, 79Whe] display interference? Loosely speaking, the photon has started its path as a particle. Indeed, when it passed the first beam splitter it had to make a choice to travel along only one of the two arms. However, by the insertion of the beam splitter it is forced to suddenly behave as a wave. For this purpose it would have had to travel on both paths. Classical intuition tells us that the past has already decided the future of the photon: When the photon entered the interferometer the second beam splitter was absent and the photon had to take one of the two paths. Therefore, we expect no interference to occur.

In the meantime many delayed choice experiments have been performed [87All, 87Hel, 89Bal, 95Her]. They clearly *do* show interference. This counter-intuitive result confirms John Archibald Wheeler's notion: "No elementary phenomenon is a phenomenon until it is an observed phenomenon" [79Whe]. It is the idea of a photon existing as a real object before the measurement which leads us into this paradoxical situation of possible actions back into the past. The delayed choice experiment teaches us that "the past has no existence except as it is recorded in the present" [78Whe].

5.1.9.2.2 Quantum-optical tests of complementarity

Nature prevents us from obtaining complete which-path information when we try to observe also interference. But what is the mechanism that erases the information about one of the two complementary observables? Niels Bohr in his rebuttal to Albert Einstein's ingenious proposal of recoiling slits [49Boh] argues that the physical positions of the slits are only known within the uncertainty principle. This error contributes a random phase shift to the photon which erases the interference patterns. Such random phase arguments are appealing. Unfortunately, they are incomplete: In principle, and in practice, it is possible to design experiments [91Scu, 98Due] that provide which-path information via detectors without disturbing the system in any noticeable way. In this case, the loss of coherence is due to the establishing of quantum correlations.

Figure 5.1.9 displays such a which-path detector. Here we consider a double-slit experiment for atoms with a high-Q microwave resonator behind each slit. The fields are resonant with an atomic transition. The interaction time is chosen in such a way that the atom makes a transition while it traverses the resonator. In this case the field state is modified by the deposition of a single photon. When there is only one atom in the apparatus at the same time it can only deposit one single photon. This event can take place either in the upper or the lower cavity. We denote the center-of-mass wave function for the path through the upper (lower) cavity by $\phi_\mathrm{u}(\boldsymbol{r})$ $(\phi_\mathrm{l}(\boldsymbol{r}))$ and the initial field state in both cavities by $|\,\psi^{(\mathrm{i})}\,\rangle$. Hence, the initial state before the interaction reads

$$|\,\Psi^{(\mathrm{i})}(\boldsymbol{r})\,\rangle = [\phi_\mathrm{u}(\boldsymbol{r}) + \phi_\mathrm{l}(\boldsymbol{r})]\,|\,\psi_\mathrm{u}^{(\mathrm{i})}\,\rangle|\,\psi_\mathrm{l}^{(\mathrm{i})}\,\rangle|\,a\,\rangle\,. \tag{5.1.71}$$

The transition of the atom from the excited state $|\,a\,\rangle$ to the ground state $|\,b\,\rangle$ changes the field state in the respective cavity to $|\,\psi_\mathrm{u}^{(\mathrm{f})}\,\rangle$ or $|\,\psi_\mathrm{l}^{(\mathrm{f})}\,\rangle$. Thus, the final state

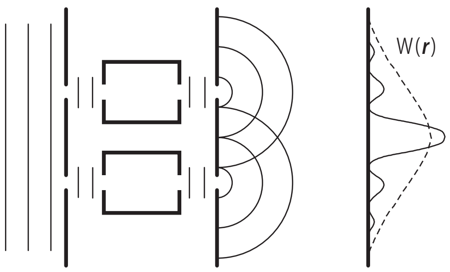

Fig. 5.1.9. Cavity fields as which-path detectors in a double-slit experiment. An atom in the excited state passing through the left double-slit can deposit its excitation in one of the two microwave cavities. The contrast of the interference structure on the screen depends on the initial field state in the cavities. A Fock state provides which-path information and no interference emerges (dashed line). For a coherent state no which-path information is available and we observe interference (solid line).

$$|\,\Psi^{(\mathrm{f})}(\boldsymbol{r})\,\rangle = \Big[\phi_{\mathrm{u}}(\boldsymbol{r})|\,\psi_{\mathrm{u}}^{(\mathrm{f})}\,\rangle|\,\psi_{\mathrm{l}}^{(\mathrm{i})}\,\rangle + \phi_{\mathrm{l}}(\boldsymbol{r})|\,\psi_{\mathrm{u}}^{(\mathrm{i})}\,\rangle|\,\psi_{\mathrm{l}}^{(\mathrm{f})}\,\rangle\Big]\,|\,b\,\rangle \tag{5.1.72}$$

of the system after the interaction reflects the fact that the center-of-mass motion is entangled with the field states. The probability $W(\boldsymbol{r})$ to find the atom at the position $\boldsymbol{r}$ independent of the cavity fields is then

$$W(\boldsymbol{r}) = |\phi_{\mathrm{u}}(\boldsymbol{r})|^2 + |\phi_{\mathrm{l}}(\boldsymbol{r})|^2 + \Big(\phi_{\mathrm{u}}(\boldsymbol{r})\phi_{\mathrm{l}}^*(\boldsymbol{r})\langle\,\psi_{\mathrm{u}}^{(\mathrm{f})}\,|\,\psi_{\mathrm{u}}^{(\mathrm{i})}\,\rangle\langle\,\psi_{\mathrm{l}}^{(\mathrm{i})}\,|\,\psi_{\mathrm{l}}^{(\mathrm{f})}\,\rangle + \mathrm{c.c.}\Big)\ . \tag{5.1.73}$$

The size of the interference term is determined by the scalar product between the initial and the final quantum states of the two cavities. When we start from a coherent state of large average photon number the addition of one photon is not changing the field significantly and the scalar product is almost unity. In this case, the amplitude of the interference terms displays a maximum. However, when we start from a Fock state in both cavities, that is a state of well-defined photon number, the addition of one photon creates another Fock state which is orthogonal to the initial field state. As a consequence the interference terms vanish. This behavior is consistent with the principle of complementarity. In the case of the Fock state we can tell the path of the atom by observing the photon deposited in the cavity. In the case of a coherent state the broad photon distribution does not allow us to observe the addition of the photon and we can not obtain path information.

We conclude by mentioning that at no place in this argument have we made use of random phase disturbances. Nevertheless, a heated discussion objecting to this point of view [94Sto] has emerged but has been decided in favor of entanglement by an experiment [98Due].

5.1.9.3 Entanglement

The state description of classical mechanics is deeply rooted in our experience trained by a macroscopic world. Indeed, the state of any mechanical system in classical physics is completely determined when we specify or measure positions and momenta of all particles involved. As a consequence, a classical state describes deterministically all properties of each single particle in the total system. Moreover, this information on any single part of a classical ensemble does not depend on what measurements are to be performed on the other parts. This property reflects the typical local and realistic character of classical physics. Even though we have described it here for classical mechanics, it can be stated equally well for other classical branches of physics such as electrodynamics and thermodynamics.

Quantum theory strongly challenges this classical picture of our world. A quantum state is defined by a vector $|\,\Psi\,\rangle$ in Hilbert space. Characteristic properties of a quantum system can be entangled between its different subsystems. None of the subsystems alone usually suffices to measure these properties, since the results of the measurements depend on the observable that is measured at the other subsystems.

This amazing peculiarity of the quantum-mechanical state description was first clearly expressed and criticized in the famous paper [35Ein] by Albert Einstein, Boris Podolsky and Nathan Rosen (EPR). Their gedanken experiment shows that the quantum mechanics of entangled systems contains elements that are in conflict with a local and realistic view. EPR concluded that quantum mechanics must be an incomplete theory which one day should be replaced by a deeper theory based on further still unrecognized variables, the so-called hidden variables. The word "entanglement" itself was first used by Erwin Schrödinger in yet another famous paper [35Sch] of the year 1935.

5.1.9.4 Bell inequality

In 1964 John S. Bell studied the most general consequences of such a hidden-variable theory or Local Realistic Theory (LRT). He realized [64Bel] that the requirements of a LRT impose strong limitations on the possible correlations between the subparts of a two-particle system. The quantitative formulation of these limits is given by the famous Bell inequalities which are the topic of the present section [78Cla, 93Mer, 01Wer].

We imagine the most elementary composite system which consists of only two particles each of which has two distinguishable properties. That is, each particle can be described by a dichotomic variable. We stipulate that these correlated particles, after being prepared by a source Q, are sent to two separated observers A and B. A LRT assumes that the measurements of observers A and B are fully described by observables $a(\boldsymbol{\alpha}, \lambda)$ and $b(\boldsymbol{\beta}, \lambda)$ which depend locally on the chosen measurement parameters $\boldsymbol{\alpha}$ and $\boldsymbol{\beta}$ as well as on the hidden variables λ.

The value of such an observable is determined when we specify $\boldsymbol{\alpha}$ or $\boldsymbol{\beta}$ and λ. Moreover, since we have simply assumed dichotomic properties we can denote these values by ± 1. When each observer tunes his apparatus to two directions $\boldsymbol{\alpha}_i$ and $\boldsymbol{\beta}_i$ $(i = 1, 2)$ we have

$$|(a_1 + a_2)\, b_1 + (a_1 - a_2)\, b_2| = 2 \tag{5.1.74}$$

with the abbreviations $a_i \equiv a(\boldsymbol{\alpha}_i, \lambda)$ and $b_i \equiv b(\boldsymbol{\beta}_i, \lambda)$.

Equation (5.1.74) holds true for any given hidden-variable set λ. If the source Q emits correlated particles described by a certain normalized distribution $\rho(\lambda)$ we immediately find

$$\left| \int_{\Lambda} \mathrm{d}\lambda\, \rho(\lambda)\, [(a_1 + a_2)\, b_1 + (a_1 - a_2)\, b_2] \right| \le 2 \tag{5.1.75}$$

or using the LRT correlation functions

$$\langle a_i b_j \rangle_{\mathrm{LRT}} \equiv \int_{\Lambda} \mathrm{d}\lambda\, \rho(\lambda) a(\boldsymbol{\alpha}_i, \lambda) b(\boldsymbol{\beta}_j, \lambda) \tag{5.1.76}$$

we arrive at the Bell inequality

$$|\langle a_1 b_1 \rangle_{\mathrm{LRT}} + \langle a_2 b_1 \rangle_{\mathrm{LRT}} + \langle a_1 b_2 \rangle_{\mathrm{LRT}} - \langle a_2 b_2 \rangle_{\mathrm{LRT}}| \le 2\,. \tag{5.1.77}$$

This inequality limits the correlations that can be described within a LRT. It is important to emphasize that inequalities of this type have nothing to do with quantum mechanics.

However, we may ask for the quantum-mechanical predictions for possible correlations between dichotomic observables of two systems. In fact, two-level systems (e.g. spin $\frac{1}{2}$-systems) are dichotomic and the corresponding operator for a system A (B) is given by $\hat{a}(\boldsymbol{\alpha}) \equiv \boldsymbol{\alpha} \cdot \hat{\boldsymbol{\sigma}}$ ($\hat{b}(\boldsymbol{\beta}) \equiv \boldsymbol{\beta} \cdot \hat{\boldsymbol{\sigma}}$) with the usual Pauli operator $\hat{\boldsymbol{\sigma}} \equiv (\hat{\sigma}_x, \hat{\sigma}_y, \hat{\sigma}_z)$, (5.1.43). The unit vector $\boldsymbol{\alpha}$ ($\boldsymbol{\beta}$) describes the measurement direction. If two systems A and B are prepared in a quantum state $|\,\Psi\,\rangle_{AB}$ the corresponding correlations are given by

$$\langle\,\Psi\,|\,\hat{a}(\boldsymbol{\alpha}_i)\hat{b}(\boldsymbol{\beta}_j)\,|\,\Psi\,\rangle \equiv \langle\,\hat{a}_i\hat{b}_j\,\rangle_{\mathrm{QM}}\,. \tag{5.1.78}$$

Hence we can construct the same sum of correlation functions as in (5.1.77). When we calculate this sum for the *entangled* singlet state

$$|\,\Psi\,\rangle_{AB} = \frac{1}{\sqrt{2}}\Big(|\uparrow\rangle_A|\downarrow\rangle_B - |\downarrow\rangle_A|\uparrow\rangle_B\Big) \tag{5.1.79}$$

and the measurement directions $\boldsymbol{\alpha}_1 = (0, 0, 1)$, $\boldsymbol{\alpha}_2 = (1, 0, 0)$, $\boldsymbol{\beta}_1 = (1/\sqrt{2}, 0, 1/\sqrt{2})$, and $\boldsymbol{\beta}_2 = (-1/\sqrt{2}, 0, 1/\sqrt{2})$ we arrive at

$$\Big|\langle\,\hat{a}_1\hat{b}_1\,\rangle_{\mathrm{QM}} + \langle\,\hat{a}_2\hat{b}_1\,\rangle_{\mathrm{QM}} + \langle\,\hat{a}_1\hat{b}_2\,\rangle_{\mathrm{QM}} - \langle\,\hat{a}_2\hat{b}_2\,\rangle_{\mathrm{QM}}\Big| = 2\sqrt{2}\,. \tag{5.1.80}$$

Consequently, quantum mechanics allows for correlations that are stronger than the ones in any local realistic theory. The essential question now is whether dichotomic microsystems provided by nature show two-particle correlations that agree with the predictions of a LRT, (5.1.77) or with those of quantum mechanics, (5.1.80). A variety of such Bell-type experiments have been performed in the past with ever increasing accuracy [82Asp, 92Bre, 98Wei, 01Row]. They all support the quantum result, (5.1.80), and lead to the fundamental conclusion that quantum mechanics is a nonlocal and nonrealistic, but correct description of nature.

5.1.10 New frontiers

The material presented in the preceding sections defines the classical topics of quantum optics. We dedicate the final section of this review to a summary of recent developments in three newly emerging and rapidly moving fields of quantum optics: atom optics, Bose–Einstein condensation and quantum information.

5.1.10.1 Atom optics in quantized fields

One prediction of quantum mechanics is the wave nature of massive particles, that is we can associate a de Broglie matter wave with their center-of-mass motion. Due to its similarities to light optics this branch of atomic physics is called atom optics. In Sect. 5.1.4 we have derived the Hamiltonian, (5.1.46), describing the quantum dynamics of a two-level atom interacting with a quantized light field. Since this Hamiltonian also includes the center-of-mass motion we now briefly outline some consequences of this theory.

In the interaction of an atom with quantized light the roles of matter and light are interchanged. Indeed, classically atoms are treated as particles and light as waves. However, we now bring out the wave nature of matter and the particle nature of light. This combination has opened a new field namely atom optics in quantized light fields [90Kaz, 97Her, 99Fre, 01Mey] which is the marriage of the two fields atom optics and cavity quantum electrodynamics.

The state vector

$$|\,\Phi(t)\,\rangle = \sum_{n=0}^{\infty} \int \mathrm{d}V\ [\Phi_{a,n-1}(\boldsymbol{R},t)|\,a,n-1\,\rangle + \Phi_{b,n}(\boldsymbol{R},t)|\,b,n\,\rangle]\ |\,\boldsymbol{R}\,\rangle \tag{5.1.81}$$

describes the combined system of the center-of-mass motion, internal states of a resonant two-level atom and the states of the electromagnetic field. Its time dependence follows from the Schrödinger equation

$$\mathrm{i}\hbar\frac{\partial}{\partial t}\Phi_n^{(\pm)}(\boldsymbol{R},t) = \left[\frac{\hat{\boldsymbol{P}}^2}{2M} + U_n^{(\pm)}(\boldsymbol{R})\right]\ \Phi_n^{(\pm)}(\boldsymbol{R},t) \tag{5.1.82}$$

with the help of the Hamiltonian, (5.1.46). Here we have introduced the dressed-state amplitudes $\Phi_n^{(\pm)} \equiv (\Phi_{b,n} \pm \Phi_{a,n-1})/\sqrt{2}$ and have defined the potentials

$$U_n^{(\pm)}(\boldsymbol{R}) \equiv \pm\wp\cdot\boldsymbol{u}(\boldsymbol{R})\,\mathcal{E}_0\sqrt{n}\,. \tag{5.1.83}$$

Hence the probability amplitudes $\Phi_n^{(\pm)}$ satisfy a Schrödinger equation corresponding to a particle of mass M moving in the potentials $U_n^{(\pm)}$. These potentials are formed by the scalar product between

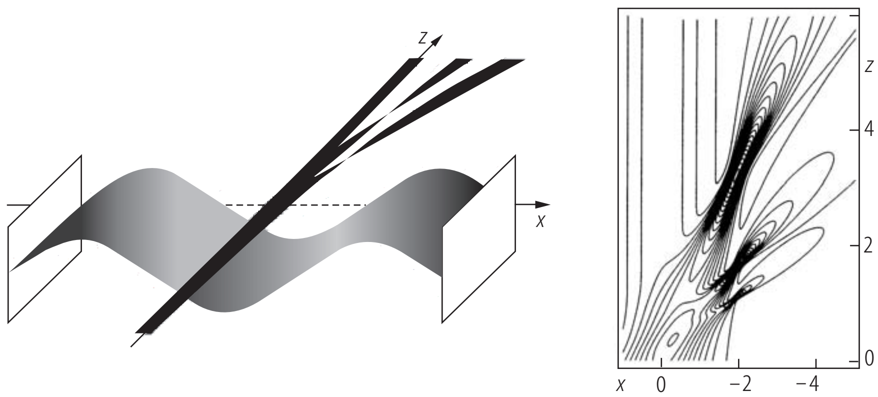

Fig. 5.1.10. A beam of resonant atoms propagating initially along the z-axis interacts with the light field in a rectangular cavity (left). Different Fock states deflect atoms in different directions and focus them at different points. This effect stands out most clearly in the contour plot (right) of the probability of finding an atom at the point with coordinates x and z. The Gaussian atomic beam centered at $x = 0$ leaves the cavity at $z = 0$. The field is in a coherent state of average photon number $\langle \hat{n} \rangle = 1$. The undeflected and unfocused partial wave associated with the cavity vacuum state represents the profile of the incident beam. The deflected partial waves associated with different photon states of the field focus at different points.

the dipole moment $\wp$ and the mode function $\boldsymbol{u}(\boldsymbol{R})$. Moreover, they scale with the vacuum electric field strength $\mathcal{E}_0$ and the square root of the photon number. Since the photon number n can only assume integer values we obtain a discrete set of potentials. Hence the granular structure of the radiation field manifests itself in a discrete superposition of potentials.

We can already gain a basic understanding of the corresponding effects by using a classical picture. The atom in each single potential feels a force that is proportional to the gradient of the potential. This force manifests itself in a deflection of atoms which is maximal when the atom starts at a node of the mode function. For a quantized field in a coherent state for example we have a discrete superposition of number states which translates into a discrete set of deflected beams [92Her] as shown in Fig. 5.1.10.

At an anti-node there is no force since the gradient vanishes. Nevertheless, quantum-mechanically there is an effect on the wave packet: The appropriate quadratic potential acts as a lens. Due to the superposition of potentials of discrete steepnesses we find a superposition of foci – a quantum lens [94Ave].

Unfortunately, so far no experimental results for the deflection of atoms in quantized fields are available yet. However, deflection [92Sle1], focusing [92Sle2] and interferometry [95Ras] of atomic de Broglie waves due to a *classical* light field has been demonstrated experimentally. This case follows from (5.1.82) in the limit of a single photon number state $|\, n_0 \,\rangle$, where we have only a single potential $U_{n_0}^{(\pm)}$ and n_0 is determined by the intensity of the classical light field.

5.1.10.2 Bose–Einstein condensation

Even more interesting is the case when the de Broglie wavelength of the atoms becomes of the order of their separation. Then the individual atoms loose their identity and their wave functions start to overlap. In the case of bosonic atoms there exists Bose–Einstein condensation where the atoms are in the ground state of the relevant Hamiltonian.

5.1.10.2.1 History

In 1924 Satyendra Nath Bose [24Bos] published his calculations on statistical properties of particles which are now known as bosons. More precisely, he presented an alternative derivation of Planck's radiation law. Albert Einstein [24Ein, 25Ein] extended this work to massive particles and predicted a phase transition in an ideal gas consisting of massive bosons – the famous Bose–Einstein condensation, where the ground state of the system becomes macroscopically occupied. Weakly interacting Bose gases were investigated by Nikolai N. Bogoliubov in 1947 [47Bog]. He showed that Bose–Einstein condensation was not much altered by weak interactions. However, the long-wavelength response of a Bose–Einstein condensate consisting of weakly interacting particles is completely different from an ideal gas.

In 1938 Fritz London suggested that Bose–Einstein condensation is responsible for the superfluidity of liquid ^{4}He [38Lon]. However, due to the strong interactions between the atoms, only a small fraction of ^{4}He atoms are condensed as has been observed in neutron scattering experiments later on. Superfluid ^{4}He was therefore never accepted as a convincing proof for Bose–Einstein condensation. Other systems, where evidence for Bose–Einstein condensation was found, are excitons in optically pumped semiconductors [93Lin]. Experiments with spin-polarized atomic hydrogen started already in 1980 [80Sil], but Bose–Einstein condensation was achieved only recently [98Fri]. In 1995 clear evidence of Bose–Einstein condensation was found in dilute atomic gases consisting of alkali atoms [95And, 95Bra, 95Dav].

For a review on Bose–Einstein condensation in atomic gases, see the proceedings of the 1998 Varenna summer school [99Ing] and a collection of articles on ultracold matter in Nature (Nature **416** (2002) 205–246) [02Ang, 02Bur, 02Chu, 02Mon, 02Rol, 02Ude]. An overview of the theory of Bose-condensed atomic gases can be found in several review articles [98Par, 99Dal, 01Leg, 02Ste] and text books [01Mey, 01Pet, 03Pit].

5.1.10.2.2 Bose–Einstein condensation in dilute atomic gases

Roughly speaking, the condition for Bose–Einstein condensation is that the de Broglie wavelength of the atoms becomes comparable to the average distance between the atoms. When we want to have Bose–Einstein condensation in a dilute gas we therefore have to cool the atoms, that is increase their de Broglie wavelength.

In order to achieve Bose–Einstein condensation for gases with current technology two steps are necessary. First the atoms are trapped in a magneto-optical trap and cooled by lasers [92Dal, 01Bar, 02Met]. It turned out that this step is not sufficient to reach the condition for Bose–Einstein condensation. Therefore, the atoms are transformed into a purely magnetic trap and evaporative cooling is used to finally achieve Bose–Einstein condensation. Evaporative cooling requires collisions between the atoms. These collisions, however, open other decay channels for trapped atoms, for example formation of molecules via three-body collisions. Therefore, it is not obvious which elements are promising candidates for Bose–Einstein condensation. It turned out that ^{23}Na and ^{87}Rb are particularly good species to achieve Bose–Einstein condensation. These elements are now widely used to generate Bose–Einstein condensates consisting of several million atoms. Another element worth mentioning is ^{4}He for which a Bose–Einstein condensate consisting of a dilute gas of helium atoms in the 2^3S_1 metastable state has been observed [01Per].

5.1.10.2.3 Gross–Pitaevskii equation

Many properties of Bose–Einstein condensates well below the transition temperature, in particular interference effects and dynamical properties, can be explained with the help of the Gross–Pitaevskii equation [61Gro, 61Pit, 63Gro]

$$\mathrm{i}\hbar\frac{\partial}{\partial t}\psi(\boldsymbol{r},t) = \left(-\frac{\hbar^2}{2M}\Delta + V(\boldsymbol{r}) + \frac{4\pi\hbar^2 a}{M}|\psi(\boldsymbol{r},t)|^2\right)\psi(\boldsymbol{r},t) \quad (5.1.84)$$

or its time-independent version. Here $\psi(\boldsymbol{r},t)$ is the macroscopic wave function of the condensate normalized to the number of particles, $V(\boldsymbol{r})$ is the trap potential (usually a harmonic potential), and a is the s-wave scattering length which takes into account the interaction between the atoms. For repulsive interaction a is positive whereas it is negative for attractive interaction. For homogeneous systems, that is $V(\boldsymbol{r}) = 0$, equations of this type have already been studied intensively in the 1960s. In order to describe the properties of condensates generated in current experiments the influence of trap potential $V(\boldsymbol{r})$ has to be taken into account. Based on the Gross–Pitaevskii equation, collective excitations, quantized vortices, and solitons in trapped Bose–Einstein condensates were predicted.

Generalizations of the Gross–Pitaevskii equation (5.1.84) are used to describe multi-component condensates and the manipulation of internal states of the atoms via external driving fields.

For more details on the application of the Gross-Pitaevskii equation to trapped Bose-condensed atoms, see [98Par, 99Dal, 01Leg, 01Mey, 01Pet, 02Ste, 03Pit].

5.1.10.2.4 Experiments with Bose–Einstein condensates

Atom optics. The first experiments by Eric A. Cornell, Carl E. Wieman and Wolfgang Ketterle have shown that there was a phase transition in their sample. However, there was no direct proof for coherent matter waves. In another experiment [97And] interference fringes in the overlap region of two condensates were observed, a clear indication of the coherence of matter waves. Since a Bose–Einstein condensate is a source for coherent matter waves, a potential application is an atom laser, a device analogous to an optical laser which instead of light emits matter waves. The first prototype of an atom laser was realized in 1996 [97Mew]. A radio-frequency field was used to change the internal state of the atoms in such a way that they were coupled out of the trap without loosing their coherence properties. Using similar ideas, several other groups demonstrated that atom lasers based on Bose–Einstein condensates can indeed provide an intense source for coherent matter waves [98And, 99Blo, 99Hag]. These results are summarized in Fig. 5.1.11.

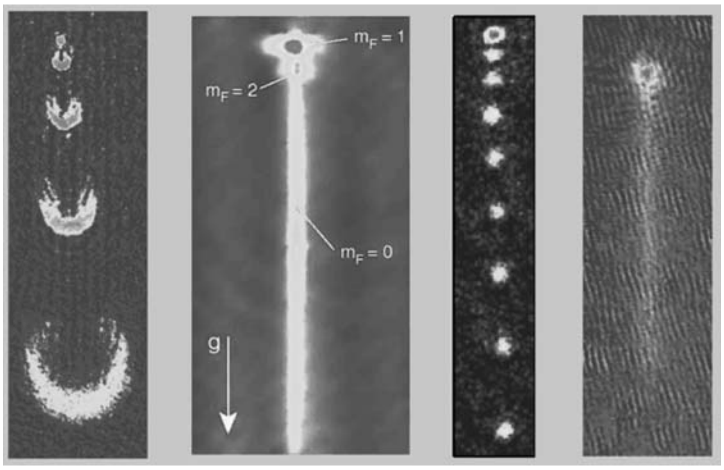

Fig. 5.1.11. Atom lasers at MIT (5 mm), MPQ (2 mm), Yale (0.5 mm), and NIST (1 mm) (left to right). In the first three figures the atoms are coupled out of the trap and move downwards under the influence of gravity. In the right figure Raman pulses transfer momentum to the atoms when they are coupled out of the trap and gravity acts perpendicular to the figure. The numbers in brackets are the heights of each image. Taken from [00Ess].

In optics the invention of the laser gave rise to nonlinear optics. A well-known effect is four-wave mixing where coherent light with a new frequency is generated. Bose–Einstein condensates as a coherent source for matter waves opened the way for nonlinear atom optics. In 1999 Deng et al. [99Den] demonstrated that it is possible to mix three matter waves to produce a fourth wave with different momentum, that is four-wave mixing.

Properties of superfluids. The theory of superfluidity predicts collective excitations, quantized vortices, and the existence of second sound in a condensate [93Gri, 99Dal, 01Pet]. Furthermore, from the nonlinear structure of the Gross–Pitaevskii equation, solitons are expected. These phenomena have been observed in various experiments after Bose–Einstein condensation in alkali vapors was achieved [96Jin, 96Mew, 99Bur, 99Mat, 00Den, 00Mad, 01Abo].

Mott insulator. Bose–Einstein condensates can be used to demonstrate a phase transition from a superfluid to a Mott insulator [02Gre]. In order to observe such a quantum phase transition a Bose–Einstein condensate consisting of atoms with repulsive interaction is loaded into a three-dimensional optical lattice generated by laser fields. Depending on the depth of the lattice potential, the atoms either form a condensate where the atoms can freely move though the lattice or a Mott insulator where they are localized at a lattice site and the motion of the atoms through the lattice is blocked. The depth of the lattice potential can easily be controlled by changing the intensity of the lasers.

We conclude our discussion of Bose–Einstein condensation by mentioning that Feshbach resonances [62Fes] can be used to control the s-wave scattering length and therefore the interaction between the atoms via external magnetic fields [98Ino]. For other experiments with Bose–Einstein condensates such as matter-wave amplification, interaction of light with Bose–Einstein condensates, multi-component condensates we refer to the literature at the end of Sect. 5.1.10.2.1 and the references therein.

5.1.10.3 Quantum information

5.1.10.3.1 Quantum teleportation

The strong and nonlocal correlations between quantum systems are not just a deep and striking fact of nature. They can be even exploited for highly non-classical tasks like quantum teleportation. It is crucial for any implementation to have a good source of entangled particles. Quantum-optical sources of polarization entangled photons [97Bou] as well as momentum entangled photons [98Bos] have been used successfully to perform quantum teleportations [93Ben] in the laboratory. Moreover, continuous variable teleportation [94Vai, 98Bra] has also been demonstrated experimentally [98Fur]. We shortly describe the basis of the corresponding protocol.

The sender, Alice, has a particle 1 in the state

$$|\,\psi\,\rangle_1 = \alpha|\,0\,\rangle_1 + \beta|\,1\,\rangle_1\,, \tag{5.1.85}$$

where the orthogonal states $|\,0\,\rangle_1$ and $|\,1\,\rangle_1$ span a two-dimensional Hilbert space with complex amplitudes α and β that are normalized, $|\alpha|^2 + |\beta|^2 = 1$. In contrast to the preceding section we have now adopted the typical notation of quantum information theory by setting $|\uparrow\rangle \equiv |\,0\,\rangle$ and $|\downarrow\rangle \equiv |\,1\,\rangle$.

Alice's aim is to send the state $|\,\psi\,\rangle_1$ to Bob, the receiver, without sending particle 1 itself. Quantum teleportation achieves this by using an ancillary pair of particles 2 and 3 prepared in the entangled state

$$|\,\Psi^-\,\rangle_{23} = \frac{1}{\sqrt{2}}\Big(|\,0\,\rangle_2|\,1\,\rangle_3 - |\,1\,\rangle_2|\,0\,\rangle_3\Big)\,. \tag{5.1.86}$$

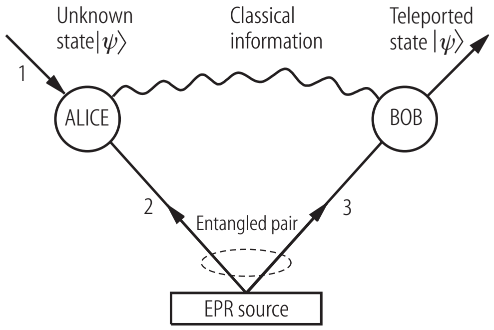

Fig. 5.1.12. Basic elements of quantum teleportation. An EPR source distributes the entangled particles 2 and 3 between Alice and Bob. Alice performs a Bell-type measurement on particle 2 and particle 1 whose state $|\,\psi\,\rangle$ will be teleported. By receiving Alice's measurement result via a classical channel Bob can in fact tune his particle to be finally in state $|\,\psi\,\rangle$.

We assume (see Fig. 5.1.12) that this pair of entangled particles stems from a common source. After preparation particle 2 is sent to Alice whereas particle 3 is kept by Bob.

The total state of all three particles reads

$$|\,\Psi\,\rangle_{123} = |\,\psi\,\rangle_1 \otimes |\,\Psi^-\,\rangle_{23} \tag{5.1.87}$$

and clearly particle 1 is neither correlated with particle 2 nor with particle 3. Formally we can, however, rewrite the total state

$$\begin{aligned}|\,\Psi\,\rangle_{123} = \frac{1}{2}\Big\{&|\,\Psi^-\,\rangle_{12}\Big(-\alpha|\,0\,\rangle_3 - \beta|\,1\,\rangle_3\Big) + |\,\Psi^+\,\rangle_{12}\Big(-\alpha|\,0\,\rangle_3 + \beta|\,1\,\rangle_3\Big)\\ &+|\,\Phi^-\,\rangle_{12}\Big(\alpha|\,1\,\rangle_3 + \beta|\,0\,\rangle_3\Big) + |\,\Phi^+\,\rangle_{12}\Big(\alpha|\,1\,\rangle_3 - \beta|\,0\,\rangle_3\Big)\Big\}\end{aligned} \tag{5.1.88}$$

using the orthogonal Bell-basis states

$$|\,\Psi^\pm\,\rangle_{12} = \frac{1}{\sqrt{2}}\Big(|\,0\,\rangle_1|\,1\,\rangle_2 \pm |\,1\,\rangle_1|\,0\,\rangle_2\Big), \quad |\,\Phi^\pm\,\rangle_{12} = \frac{1}{\sqrt{2}}\Big(|\,0\,\rangle_1|\,0\,\rangle_2 \pm |\,1\,\rangle_1|\,1\,\rangle_2\Big) \tag{5.1.89}$$

for particles 1 and 2 owned by Alice. She can now perform a Bell-state measurement and thereby project the state $|\,\Psi\,\rangle_{123}$, (5.1.88), on one of the four states, (5.1.89). As a result of this measurement Bob's particle 3 will be prepared in one of the states directly related to Alice's result according to (5.1.88). For example, if Alice finds the result Φ^-, Bob's particle will be in state $\alpha|\,1\,\rangle_3 + \beta|\,0\,\rangle_3$ which looks similar to the original state, (5.1.85), but the basis states are flipped. This flip can be repaired by Bob with a simple unitary transformation $\hat{U}_{\Phi^-} = \hat{\sigma}_x = |\,0\,\rangle\langle\,1\,| + |\,1\,\rangle\langle\,0\,|$. This works similarly for all four measurement results that Alice can get. All that Alice has to do is to inform Bob via a classical channel about her measurement result. This enables him to choose the correct unitary transformation from the four possible ones: $\hat{U}_{\Psi^-} = \mathbb{1}$, $\hat{U}_{\Psi^+} = \hat{\sigma}_z = |\,0\,\rangle\langle\,0\,| - |\,1\,\rangle\langle\,1\,|$, $\hat{U}_{\Phi^-} = \hat{\sigma}_x = |\,0\,\rangle\langle\,1\,| + |\,1\,\rangle\langle\,0\,|$, and finally $\hat{U}_{\Phi^+} = \hat{\sigma}_y = i(|\,1\,\rangle\langle\,0\,| - |\,0\,\rangle\langle\,1\,|)$. After applying this transformation he obtains the state $|\,\psi\,\rangle_3 = \alpha|\,0\,\rangle_3 + \beta|\,1\,\rangle_3$ up to an overall phase and hence teleportation is completed.

This is a perfect example how quantum information can be sent with the help of entanglement. Moreover, it is also possible to transmit classical information (classical bits) by using entangled states between the communicating parties. The corresponding protocols of the so-called quantum dense coding [92Ben2, 96Mat] even show that this can be done more effectively than with any imaginable classical approach. This clearly shows the fascinating properties of quantum systems that can be prepared and controlled with quantum-optical means.

Another example for the far-reaching prospects of quantum information processing is quantum cryptography which we describe in the next paragraph.

5.1.10.3.2 Quantum cryptography

Secret messages are only as secure as the keys used to encrypt them. Classical cryptography has developed fascinating methods to encode a message using certain keys, but it has no means to ensure absolute security of those keys. Quantum cryptography closes this gap by showing how to generate and simultaneously exchange a secure key based on the laws of quantum physics.

The basic idea is that in quantum mechanics any measurement process changes the properties of a system. Consequently, whatever strategy an eavesdropper (normally called Eve) chooses, she will leave a trace on the quantum objects that are used for transmitting a key. This trace can be detected by the sender (typically known as Alice) and the intended recipient (usually called Bob).

In order to understand this in more detail we shall discuss a particular protocol for quantum key generation and distribution known as B92 protocol [84Ben, 91Eke, 92Ben1]. The quantum objects used for the transmission of the key are two-level systems (e.g. spin $\frac{1}{2}$) with basis states $|\uparrow\rangle$ and $|\downarrow\rangle$. They are defined by the eigenvalue equations

$$\hat{\sigma}_z|\uparrow\rangle = +|\uparrow\rangle\,, \quad \hat{\sigma}_z|\downarrow\rangle = -|\downarrow\rangle \tag{5.1.90}$$

of the $\hat{\sigma}_z$ Pauli operator with eigenvalues ± 1. In addition we need the superposition states

$$|\rightarrow\rangle \equiv \frac{1}{\sqrt{2}}\left(|\uparrow\rangle + |\downarrow\rangle\right)\,, \quad |\leftarrow\rangle \equiv \frac{1}{\sqrt{2}}\left(|\uparrow\rangle - |\downarrow\rangle\right) \tag{5.1.91}$$

which fulfill the eigenvalue equations

$$\hat{\sigma}_x|\rightarrow\rangle = +|\rightarrow\rangle\,, \quad \hat{\sigma}_x|\leftarrow\rangle = -|\leftarrow\rangle\,. \tag{5.1.92}$$

of the $\hat{\sigma}_x$ Pauli operator. In the B92 protocol Alice now generates a random bit sequence and encodes it on her quantum objects by sending $|\uparrow\rangle$ if the bit reads $a = 0$ and by sending $|\rightarrow\rangle$ if the bit reads $a = 1$. Also Bob prepares a purely random list of bits. According to this list he measures Alice's quantum objects. He chooses the $\hat{\sigma}_z$ basis if his bit reads $b = 1$ and the $\hat{\sigma}_x$ basis if his bit reads $b = 0$. Clearly he can find the eigenvalue $+1$ for all four possible bit combinations a and b, but the value -1 he can only find with 50% probability if the bit combination was $a = b = 0$ or $a = b = 1$. Bob will never record a -1 when his bit is different from Alice's. For the values -1 the bits in the two lists are therefore completely correlated. Hence in the final step of the B92 protocol Bob simply sends a copy of his measurement *results* to Alice (*not* the measurement basis). He may even send this over a public channel. Alice and Bob then only keep those bits in their lists that correspond to a -1 measurement result. The sequence of these *key bits* forms two identical and completely random keys.

Moreover, they can check their lists for an eavesdropper by sacrifying some of their key bits and comparing them. Let us assume that Eve makes her own measurement on Alice's quantum particles in the $\hat{\sigma}_x$ or $\hat{\sigma}_z$ basis and sends on the results to Bob. If, for example, Alice has prepared a $|\uparrow\rangle$ object ($a = 0$) and Eve wrongly chooses the $\hat{\sigma}_x$ basis, she might find $|\rightarrow\rangle$ and send it to Bob. Hence Eve has disturbed the properties of the original quantum object and left a trace by her quantum measurement process. If Bob applies a $\hat{\sigma}_z$ basis ($b = 1$) he might read of the value -1 with 50% probability, even though the bit combination was $a = 0$ and $b = 1$. Therefore, Alice and Bob can use sufficiently many of their key bits and check for $a = 0$ and $b = 1$ or $a = 1$ and $b = 0$ combinations. If the rate of such results is high, they know that an eavesdropper was present and consequently they have to discard the complete key. We emphasize that a general analysis of eavesdropping strategies is quite complicated [98Bih, 99Lo, 00Nie, 00Sho, 01May] and not even completely carried through for all possible protocols. Nevertheless, the technology for achieving quantum cryptography in practice [95Hug, 96Mul, 02Hug, 02Stu] is already highly developed and even stands at the edge of being commercialized.

References for 5.1

1802You Young, Th.: Philos. Trans. R. Soc. (London) **92** (1802) 12.

1873Max Maxwell, J.C.: A treatise on electricity and magnetism, 2 Vols., Oxford: Clarendon Press, 1873.

1900Pla Planck, M.: Verh. Dtsch. Phys. Ges. **2** (1900) 202.

1901Pla Planck, M.: Ann. Phys. (Leipzig) **4** (1901) 553.

1904Tho Thomson, J.J.: Philos. Mag. **7** (1904) 237.

1905Ein Einstein, A.: Ann. Phys. (Leipzig) **17** (1905) 132.

17Ein Einstein, A.: Phys. Z. **18** (1917) 121.

24Bos Bose, S.: Z. Phys. **26** (1924) 178.
24Ein Einstein, A.: Sitzungsber. K. Preuss. Akad. Wiss. **1924** (1924) 261.
24Wen Wentzel, G.: Z. Phys. **22** (1924) 193.

25Bor1 Born, M.: Atommechanik, Berlin: Springer-Verlag, 1925.
25Bor2 Born, M., Heisenberg, W., Jordan, P.: Z. Phys. **35** (1925) 557.
25Bor3 Born, M., Jordan, P.: Z. Phys. **34** (1925) 858.
25Ein Einstein, A.: Sitzungsber. K. Preuss. Akad. Wiss. **1925** (1925) 3.
25Hei Heisenberg, W.: Z. Phys. **33** (1925) 879.

26Lew Lewis, G.N.: Nature (London) **118** (1926) 874.
26Pau Pauli, W., in: Handbuch der Physik XXIII, Geiger, H., Scheel, K., (eds.), Berlin: Springer-Verlag, 1926, 1.
26Sch1 Schrödinger, E.: Ann. Phys. (Leipzig) **79** (1926) 734.
26Sch2 Schrödinger, E.: Naturwissenschaften **14** (1926) 664.

27Dir Dirac, P.A.M.: Proc. R. Soc. (London) A **114** (1927) 243.
27Jor Jordan, P.: Z. Phys. **40** (1927) 661.

28Boh Bohr, N.: Nature (London) **121** (1928) 580.

30Bor Born, M., Jordan, P.: Elementare Quantenmechanik, Heidelberg: Springer-Verlag, 1930.

31Wei von Weizsäcker, C.F.: Z. Phys. **70** (1931) 114.

32Fer Fermi, E.: Rev. Mod. Phys. **4** (1932) 87.

33Boh Bohr, N., Rosenfeld, L.: Mat. Fys. Medd. K. Dan. Vidensk. Selsk. **12** (8) (1933).

35Dir Dirac, P.A.M.: The principles of quantum mechanics, Oxford: Clarendon Press, 1935.
35Ein Einstein, A., Podolsky, B., Rosen, N.: Phys. Rev. **47** (1935) 777.
35Sch Schrödinger, E.: Naturwissenschaften **23** (1935) 807; 823; 844.

38Lon London, F.: Nature (London) **141** (1938) 643.

41Wei von Weizsäcker, C.F.: Z. Phys. **118** (1941) 489.

47Bog Bogoliubov, N.N.: J. Phys. USSR **11** (1947) 23.
47Lam Lamb, W.E., Retherford, R.C.: Phys. Rev. **72** (1947) 241.

49Boh Bohr, N., in: Albert Einstein: Philosopher-Scientist, Schilpp, P.A. (ed.), Evanston: Library of Living Philosophers, 1949, 200.
49Kro Kroll, N.M., Lamb, W.E.: Phys. Rev. **75** (1949) 388.

50Boh Bohr, N., Rosenfeld, L.: Phys. Rev. **78** (1950) 794.

52Sch1 Schrödinger, E.: Brit. J. Philos. Sci. **3** (1952) 109.
52Sch2 Schrödinger, E.: Brit. J. Philos. Sci. **3** (1952) 233.

56Han Hanbury Brown, R., Twiss, R.Q.: Nature (London) **177** (1956) 27.

58Boh Bohr, N.: Atomic physics and human knowledge, New York: Wiley, 1958.

61Gro Gross, E.P.: Nuovo Cimento **20** (1961) 454.
61Pit Pitaevskii, L.P.: Zh. Eksp. Teor. Fiz. **40** (1961) 646; Sov. Phys. JETP (English Trans.) **13** (1961) 451.

62Fes Feshbach, H.: Ann. Phys. (New York) **19** (1962) 287.

63Gla1 Glauber, R.J.: Phys. Rev. **130** (1963) 2529.
63Gla2 Glauber, R.J.: Phys. Rev. **131** (1963) 2766.
63Gro Gross, E.P.: J. Math. Phys. N.Y. **4** (1963) 195.
63Jay Jaynes, E.T., Cummings, F.W.: Proc. IEEE **51** (1963) 89.
63Pau Paul, H.: Ann. Phys. (Leipzig) **11** (1963) 411.
63Sud Sudarshan, E.C.G.: Phys. Rev. Lett. **10** (1963) 277.

64Bel Bell, J.S.: Physics **1** (1964) 195.
64Bor Born, M., Wolf, E.: Principles of optics, Oxford: Pergamon Press, 1964.

65Bur Burshtein, A.I.: Zh. Eksp. Teor. Fiz. **49** (1965) 1362; Sov. Phys. JETP (English Trans.) **22** (1966) 939.
65Gla Glauber, R.J., in: Qantum optics and electronics, DeWitt C., Blandin, A., Cohen-Tannoudji, C. (eds.), New York: Gordon and Breach, 1965, 331.

66Lax Lax, M., in: Brandeis University Summer Institute Lectures, Chretin, M., Gross, E.P., Deser, S. (eds.), Vol. 2., New York: Gordon and Breach, 1966.

68Car Carruthers, P., Nieto, M.M.: Rev. Mod. Phys. **40** (1968) 411.

69Cah Cahill, K.E., Glauber, R.J.: Phys. Rev. A **177** (1969) 1882.
69Mol Mollow, B.R.: Phys. Rev. **188** (1969) 1969.

70Man Mandel, L., Wolf, E. (eds.): Selected papers on coherence and fluctuations of light, Vol. I and II, New York: Dover Publications, 1970.

73Lou Louisell, W.H.: Quantum statistical properties of radiation, New York: Wiley, 1973.

74Sar Sargent, M. III., Scully, M.O., Lamb, W.E.: Laser Theory, Massachusetts: Addison-Wesley, Reading, 1974.
74Sch Schuda, F., Stroud jr., C.R., Hercher, M.: J. Phys. B **7** (1974) L198.

75Deh Dehmelt, H.: Bull. Am. Phys. Soc. **20** (1975) 60.
75Wu Wu, F.Y., Grove, R.E., Ezekiel, S.: Phys. Rev. Lett. **35** (1975) 1426.

76Car1 Carmichael, H.J., Walls, D.F.: J. Phys. B **9** (1976) 1199.
76Car2 Carmichael, H.J., Walls, D.F.: J. Phys. B **9** (1976) L43.
76Har Hartig, W., Rasmussen, W., Schieder, R., Walther, H.: Z. Phys. A **278** (1976) 205.

77Kim Kimble, H.J., Dagenais, M., Mandel, L.: Phys. Rev. Lett. **39** (1977) 691.
78Cla Clauser, J.F., Shimony, A.: Rep. Prog. Phys. **41** (1978) 1881.
78Kim Kimble, H.J., Dagenais, M., Mandel, L.: Phys. Rev. A **18** (1978) 201.
78Whe Wheeler, J.A., in: Mathematical foundations of quantum theory, Marlow, A.R. (ed.), New York: Academic Press, 1978.

79Pau Pauli, W., in: Wissenschaftlicher Briefwechsel mit Bohr, Einstein, Heisenberg u.a., Vol. I, Hermann, A., von Meyenn, K., Weisskopf, V.F. (eds.), New York: Springer, 1979.
79Whe Wheeler, J.A., in: Problems in the foundations of physics, International School of Physics "Enrico Fermi", Course LXXII, Amsterdam: North-Holland, 1979.

80Sil Silvera, I.F., Walraven, J.T.M.: Phys. Rev. Lett. **44** (1980) 164.

82Asp Aspect, A., Dalibard, J., Roger, G.: Phys. Rev. Lett. **49** (1982) 1804.
82Cre Cresser, J.D., Häger, J., Leuchs, G., Rateike, M., Walther, H., in: Dissipative systems in quantum optics, Bonifacio, R., Lugiato, L. (eds.), Topics in Current Physics Vol. 27, Berlin: Springer-Verlag, 1982, 21.

83Ber Bertolotti, M.: Masers and lasers. An historical approach, Bristol: Adam Hilger Ltd, 1983.
83Whe Wheeler, J.A., Zurek, W.H. (eds.): Quantum theory and measurement, Princeton: Princeton University Press, 1983.

84Ben Bennett, C.H., Brassard, G., in: Proc. IEEE Int. Conference on Computers, Systems and Signal Processing, Los Alamitos: IEEE Press, 1984.
84Hak Haken, H.: Laser theory, Heidelberg: Springer-Verlag, 1984.
84Hil Hillery, M., O'Connell, R.F., Scully, M.O., Wigner, E.P.: Phys. Rep. **106** (1984) 121.

85Gar Gardiner, C.W.: Handbook of stochastic methods, Berlin: Springer-Verlag, 1985.
85Mes Meschede, D., Walther, H., Müller, G.: Phys. Rev. Lett. **54** (1985) 551.
85Slu Slusher, R.E., Hollberg, L.W., Yurke, B., Mertz, J.C., Valley, J.F.: Phys. Rev. Lett. **55** (1985) 2409.

86Ber Bergquist, J.C., Hulet, R.G., Itano, W.M., Wineland, D.J.: Phys. Rev. Lett. **57** (1986) 1699.
86Fil Filipowicz, P., Javanainen, J., Meystre, P.: Phys. Rev. A **34** (1986) 3077.
86Gar Gardiner, C.W.: Phys. Rev. Lett. **56** (1986) 1917.
86Gra Grangier, P., Roger, G., Aspect, A.: Europhys. Lett. **1** (1986) 173.
86Nag Nagourney, W., Sandberg, J., Dehmelt, H.: Phys. Rev. Lett. **56** (1986) 2797.
86Sau Sauter, Th., Neuhauser, W., Blatt, R., Toschek, P.E.: Phys. Rev. Lett. **57** (1986) 1696.

87All Alley, C.O., Jakubowicz, O.G., Wickes, W.C., in: Proceedings of the 2nd international symposium on foundations of quantum mechanics, Namiki, M., Ohnuki, Y., Murayama, Y., Nomura, S. (eds.), Tokyo: Physical Society of Japan, 1987.
87Hel Hellmuth, T., Walther, H., Zajonc, A., Schleich, W.P.: Phys. Rev. A **35** (1987) 2532.
87Kim Kimble, H.J., Walls, D.F. (eds.): J. Opt. Soc. Am. B **4** (10) (1987) 1449.
87Lou Loudon, R., Knight, P.L. (eds.): J. Mod. Opt. **34** (6/7) (1987) 709.
87Lug Lugiato, L.A., Scully, M.O., Walther, H.: Phys. Rev. A **36** (1987) 740.
87Sch Schleich, W.P., Wheeler, J.A.: J. Opt. Soc. Am. B **4** (1987) 1715.

88Bre Brendel, J., Schütrumpf, S., Lange, R., Martienssen, W., Scully, M.O.: Europhys. Lett. **5** (1988) 223.
88Mey Meystre, P., Rempe, G., Walther, H.: Opt. Lett. **13** (1988) 1078.

89Asp Aspect, A., Grangier, P., Roger, G.: J. Opt. **20** (1989) 119.
89Bal Baldzuhn, J., Mohler, E., Martienssen, W.: Z. Phys. B **77** (1989) 347.
89Coh Cohen-Tannoudji, C., Dupont-Roc, J., Grynberg, G.: Photons and atoms. An introduction to quantum electrodynamics, New York: Wiley, 1989.
89Peg Pegg, D.T., Barnett, S.M.: Phys. Rev. A **39** (1989) 1665.
89Ris Risken, H.: The Fokker-Planck equation, Berlin: Springer-Verlag, 1989.

90Kaz Kazantsev, A.P., Surdutovich, G.I., Yakovlev, V.P.: Mechanical action of light on atoms, Singapore: World Scientific, 1990.
90Pau Paul, W.: Rev. Mod. Phys. **62** (1990) 531.
90Rem Rempe, G., Schmidt-Kaler, F., Walther, H.: Phys. Rev. Lett. **64** (1990) 2783.
90Sho Shore, B.W.: The theory of coherent atomic excitations, New York: Wiley, 1990.

91Bre Brendel, J., Lange, R., Mohler, E., Martienssen, W.: Ann. Phys. (Leipzig) **48** (1991) 26.
91Eke Ekert, A.: Phys. Rev. Lett. **67** (1991) 661.
91Gar Gardiner, C.W.: Quantum noise, Berlin: Springer-Verlag, 1991.
91Lou Loudon, R.: The quantum theory of light, 2nd edition, Oxford: Clarendon Press, 1991.
91Mey Meystre, P., Sargent, M. III.: Elements of quantum optics, Berlin: Springer-Verlag, 1991.
91Sch Schleich, W.P., Pernigo, M., Fam Le Kien: Phys. Rev. A **44** (1991) 2172.
91Scu Scully, M.O., Englert, B.-G., Walther, H.: Nature (London) **351** (1991) 111.
91Zur Zurek, W.H.: Phys. Today **44** (1991) 36.

92Ben1 Bennett, C.H.: Phys. Rev. Lett. **68** (1992) 3121.
92Ben2 Bennett, C.H., Wiesner, S.J.: Phys. Rev. Lett. **69** (1992) 2881.
92Blo Blockley, C.A., Walls, D.F., Risken, H.: Europhys. Lett. **17** (1992) 509.
92Bre Brendel, J., Mohler, E., Martienssen, W.: Europhys. Lett. **20** (1992) 575.
92Coh Cohen-Tannoudji, C., Dupont-Roc, J., Grynberg, G.: Atom-photon interactions, New York: Wiley, 1992.
92Dal Dalibard, J., Raimond, J.-M., Zinn-Justin, J. (eds.): Fundamental systems in quantum optics. Les Houches 1990, session LIII, Amsterdam: North-Holland, 1992.
92Gia Giacobino, E., Fabre, C. (eds.): Appl. Phys. B **55** (3) (1992) 189.
92Her Herkommer, A.M., Akulin, V.M., Schleich, W.P.: Phys. Rev. Lett. **69** (1992) 3298.
92Sle1 Sleator, T., Pfau, T., Balykin, V., Carnal, O., Mlynek, J.: Phys. Rev. Lett. **68** (1992) 1996.
92Sle2 Sleator, T., Pfau, T., Balykin, V., Mlynek, J.: Appl. Phys. B **54** (1992) 375.

93Ben Bennett, C.H., Brassard, G., Crépeau, C., Jozsa, R., Peres, A., Wootters, W.K.: Phys. Rev. Lett. **70** (1993) 1895.

93Car Carmichael, H.J.: An open systems approach to quantum mechanics, Heidelberg: Springer-Verlag, 1993.
93Gri Griffin, A.: Excitations in a Bose-condensed liquid, Cambridge: Cambridge University Press, 1993.
93Hau Haubrich, D., Höpe, A., Meschede, D.: Opt. Commun. **102** (1993) 225.
93Lin Lin, J.L., Wolfle, J.P.: Phys. Rev. Lett. **71** (1993) 1222.
93Mer Mermin, N.D.: Rev. Mod. Phys. **65** (1993) 803.
93Sch Schleich, W.P., Barnett, S.M. (eds.): Quantum phase and phase dependent measurements; Phys. Scr. T **48** (1993) 5.
93Sho Shore, B.W., Knight, P.L.: J. Mod. Opt. **40** (1993) 1195.

94Ave Averbukh, I.Sh., Akulin, V.M., Schleich, W.P.: Phys. Rev. Lett. **72** (1994) 437.
94Ber Bergou, J., Hillery, M.: Phys. Rev. A **49** (1994) 1214.
94Cir Cirac, J.I., Blatt, R., Parkins, A.S., Zoller, P.: Phys. Rev. A **49** (1994) 1202.
94Moo Moore, W.: A life of Erwin Schrödinger, Cambridge: Cambridge University Press, 1994.
94Rai Raithel, G., Wagner, C., Walther, H., Narducci, L., Scully, M.O., in: Advances in Atomic, Molecular, and Optical Physics, Supplement 2: Cavity Quantum Electrodynamics, Berman, P.R. (ed.), Boston: Academic Press, 1994, 57.
94Sto Storey, E.P., Tan, S.M., Collet, M.J., Walls, D.F.: Nature (London) **367** (1994) 626.
94Vai Vaidman, L.: Phys. Rev. A **49** (1994) 1473.
94Wal Walls, D.F., Milburn, G.J.: Quantum optics, Berlin: Springer-Verlag, 1994.
94Wil Wilkens, M.: Phys. Rev. A **48** (1994) 570.

95And Anderson, M.H., Ensher, J.R., Matthews, M.R., Wieman, C.E., Cornell, E.A.: Science **269** (1995) 198.
95Bra Bradley, C.C., Sackett, C.A., Tollett, J.J., Hulet, R.G.: Phys. Rev. Lett. **75** (1995) 1687.
95Dav Davis, K.B., Mewes, M.-O., Andrews, M.R., van Druten, N.J., Durfee, D.S., Kurn, D.M., Ketterle, W.: Phys. Rev. Lett. **75** (1995) 3969.
95Her Herzog, T.J., Kwiat, P.G., Weinfurter, H., Zeilinger, A.: Phys. Rev. Lett. **75** (1995) 3034.
95Hug Hughes, R.J., Alde, D.M., Dyer, P., Luther, G.G., Morgan, G.L., Schauer, M.: Contemp. Phys. **36** (1995) 149.
95Lam Lamb, W.E.: Appl. Phys. B **60** (1995) 77.
95Man Mandel, L., Wolf, E.: Optical coherence and quantum optics, New York: Cambridge University Press, 1995.
95Ras Rasel, E.M., Oberthaler, M.K., Batelaan, H., Schmiedmayer, J., Zeilinger, A.: Phys. Rev. Lett. **75** (1995) 2633.
95Vog Vogel, W., de Matos Filho, R.L.: Phys. Rev. A **52** (1995) 4214.

96Bar Bardroff, P.J., Leichtle, C., Schrade, G., Schleich, W.P.: Phys. Rev. Lett. **77** (1996) 2198.
96Bru Brune, M., Hagley, E., Dreyer, J., Maitre, X., Maali, A., Wunderlich, C., Raimond J.M., Haroche, S.: Phys. Rev. Lett. **77** (1996) 4887.
96Eng Englert, B.-G.: Phys. Rev. Lett. **77** (1996) 2154.
96Giu Giulini, D., Joos, E., Kiefer, C., Kupsch, J., Stamatescu, I.-O., Zeh, H.D.: Decoherence and the appearance of a classical world in quantum theory, Heidelberg: Springer-Verlag, 1996.
96Jin Jin, D.S., Ensher, J.R., Matthews, M.R., Wieman, C.E., Cornell, E.A.: Phys. Rev. Lett. **77** (1996) 420.
96Mat Mattle, K., Weinfurter, H., Kwiat, P.G., Zeilinger, A.: Phys. Rev. Lett. **76** (1996) 4656.
96Mee Meekhof, D.M., Monroe, C., King, B.E., Itano, W.M., Wineland, D.J.: Phys. Rev. Lett. **76** (1996) 1796.

96Mew Mewes, M.-O., Andrews, M.R., van Druten, N.J., Kurn, D.M., Durfee, D.S., Townsend, C.G., Ketterle, W.: Phys. Rev. Lett. **77** (1996) 988.
96Mul Muller, A., Zbinden, H., Gisin, N.: Europhys. Lett. **33** (1996) 334.
96Scu Scully, M.O., Zubairy, M.S.: Quantum optics, New York: Cambridge University Press, 1996.

97And Andrews, M.R., Townsend, C.G., Miesner, H.-J., Durfee, D.S., Kurn, D.M., Ketterle, W.: Science **275** (1997) 637.
97Bou Bouwmeester, D., Pan, J.-W., Mattle, K., Eibl, M., Weinfurter, H., Zeilinger, A.: Nature (London) **390** (1997) 575.
97Buz Buzek, V., Drobný, G., Kim, M.S., Adam, G., Knight, P.L.: Phys. Rev. A **56** (1997) 2352.
97Hoe Höffges, J.T., Baldauf, H.W., Eichler, T., Helmfrid, S.R., Walther, H.: Opt. Commun. **133** (1997) 170.
97Her Herkommer, A.M., Schleich, W.P.: Comments At. Mol. Phys. **33** (1997) 145.
97Mew Mewes, M.-O., Andrews, M.R., Kurn, D.M., Durfee, D.S., Townsend, C.G., Ketterle, W.: Phys. Rev. Lett. **78** (1997) 582.
97Sch Schrade, G., Bardroff, P.J., Glauber, R.J., Leichtle, C., Yakovlev, V., Schleich, W.P.: Appl. Phys. B **64** (1997) 181.

98And Anderson, B.P., Kasevich, M. A.: Science **282** (1998) 1686.
98Bih Biham, E., Boyer, M., Brassard, G., van de Graaf, J., Mor, T.: quant-ph/9801022.
98Bos Boschi, D., Branca, S., De Martini, F., Hardy, L., Popescu, S.: Phys. Rev. Lett. **80** (1998) 1121.
98Bra Braunstein, S.L., Kimble, H.J.: Phys. Rev. Lett. **80** (1998) 869.
98Due Dürr, S., Nonn, T., Rempe, G.: Nature (London) **395** (1998) 33.
98Fri Fried, D.G., Killian, T.C., Willmann, L., Landhuis, D., Moss, S.C., Kleppner, D., Greytak, T.J.: Phys. Rev. Lett. **81** (1998) 3811.
98Fur Furusawa, A., Sorensen, J.L., Braunstein, S.L., Fuchs, C.A., Kimble, H.J., Polzik, E.S.: Science **282** (1998) 706.
98Ino Inouye, S., Andrews, M.R., Stenger, J., Miesner, H.-J., Stamper-Kurn, D.M., Ketterle, W.: Nature (London) **392** (1998) 151.
98Lu Lu, Z.H., Bali, S., Thomas, J.E.: Phys. Rev. Lett. **81** (1998) 3635.
98Par Parkins, A.S., Walls, D.F.: Phys. Rep. **303** (1998) 1.
98Wei Weihs, G., Jennewein, T., Simon, C., Weinfurter, H., Zeilinger, A.: Phys. Rev. Lett. **81** (1998) 5039.
98Win Wineland, D.J., Monroe, C., Itano, W.M., Leibfried, D., King, B.E., Meekhof, D.M.: J. Res. Natl. Inst. Stand. Technol. **103** (1998) 259.

99Blo Bloch, I., Hänsch, T.W., Esslinger, T.: Phys. Rev. Lett. **82** (1999) 3008.
99Bur Burger, S., Bongs, K., Dettmer, S., Ertmer, W., Sengstock, K., Sanpera, A., Shlyapnikov, G.V., Lewenstein, M.: Phys. Rev. Lett. **83** (1999) 5198.
99Dal Dalfovo, F., Giorgini, S., Pitaevskii, L.P., Stringari, S.: Rev. Mod. Phys. **71** (1999) 463.
99Den Deng, L., Hagley, E.W., Wen, J., Trippenbach, M., Band, Y., Julienne, P.S., Simsarian, J.E., Helmerson, K., Rolston, S.L., Phillips, W.D.: Nature (London) **398** (1999) 218.
99Fre Freyberger, M., Herkommer, A.M., Krähmer, D.S., Mayr, E., Schleich, W.P., in: Advances in Atomic, Molecular, and Optical Physics **41**, Bederson, B., Walther, H. (eds.), Boston: Academic Press, 1999, 143.
99Hag Hagley, E.W., Deng, L., Kozuma, M., Wen, J., Helmerson, K., Rolston, S.L., Phillips, W.D.: Science **283** (1999) 1706.

99Ing Inguscio, M., Stringari, S., Wieman, C.E. (eds.): Bose-Einstein condensation in atomic gases; Proceedings of the International School of Physics “Enrico Fermi”, Course CXL, Amsterdam: IOS Press, 1999.
99Lam Lamb, W.E., Schleich, W.P., Scully, M.O., Townes, C.H.: Rev. Mod. Phys. **71** (1999) 263.
99Lo Lo, H., Chan, H.F.: Science **283** (1999) 2050.
99Mat Matthews, M.R., Anderson, B.P., Haljan, P.C., Hall, D.S., Wieman, C.E., Cornell, E.A.: Phys. Rev. Lett. **83** (1999) 2498.
99Pau Paul, H.: Photonen. Eine Einführung in die Quantenoptik, Stuttgart: B. G. Teubner, 1999.
99Wei Weidinger, M., Varcoe, B.T.H., Heerlein, R., Walther, H.: Phys. Rev. Lett. **82** (1999) 3795.
99Zei Zeilinger, A.: Rev. Mod. Phys. **71** (1999) S288.

00Den Denschlag, J., Simsarian, J.E., Feder, D.L., Clark, C.W., Collins, L.A., Cubizolles, J., Deng, L., Hagley, E.W., Helmerson, K., Reinhardt, W.P., Rolston, S.L., Schneider, B.I., Phillips, W.D.: Science **287** (2000) 97.
00Ess Esslinger, T., Bloch, I., Hänsch, T.W.: Physikalische Blätter **56**(2) (2000) 47.
00Mad Madison, K.W., Chevy, F., Bretin, V., Dalibard, J.: Phys. Rev. Lett. **84** (2000) 806.
00Mya Myatt, C.J., King, B.E., Turchette, Q.A., Sackett, C.A., Kielpinski, D., Itano, W.M., Monroe, C., Wineland, D.J.: Nature (London) **403** (2000) 269.
00Nie Nielsen, M.A., Chuang, I.L.: Quantum computation and quantum information, Cambridge: Cambridge University Press, 2000.
00Sho Shor, P.W., Preskill, J.: Phys. Rev. Lett. **85** (2000) 441.
00Var Varcoe, B.T.H., Brattke, S., Weidinger, M., Walther, H.: Nature (London) **403** (2000) 743.
00Zan von Zanthier, J., Becker, Th., Eichenseer, M., Nevsky, A.Yu., Schwedes, Ch., Peik, E., Walther, H., Holzwarth, R., Reichert, J., Udem, Th., Hänsch, T.W., Pokasov, P.V., Skvortsov, M.N., Bagayev, S.N.: Opt. Lett. **25** (2000) 1729.

01Abo Abo-Shaeer, J.R., Raman, C., Vogels, J.M., Ketterle, W.: Science **292** (2001) 476.
01Bar Bardou, F., Bouchaud, J.P., Aspect, A., Cohen-Tannoudji, C.: Lévy statistics and laser cooling, Cambridge: Cambridge University Press, 2001.
01Leg Leggett, A.J.: Rev. Mod. Phys. **73** (2001) 307.
01May Mayers, D.: Journal ACM **48** (2001) 351.
01Mey Meystre, P.: Atom optics, New York: Springer-Verlag, 2001.
01Per Pereira Dos Santos, F., Léonard, J., Wang, J., Barrelet, C.J., Perales, F., Rasel, E., Unnikrishnan, C.S., Leduc, M., Cohen-Tannoudji, C.: Phys. Rev. Lett. **86** (2001) 3459.
01Pet Pethick, C.J., Smith, H: Bose-Einstein condensation in dilute gases, Cambridge: Cambridge University Press, 2001.
01Row Rowe, M.A., Kielpinski, D., Meyer, V., Sackett, C.A., Itano, W.M., Monroe, C., Wineland, D.J.: Nature (London) **409** (2001) 791.
01Sch Schleich, W.P.: Quantum optics in phase space, Weinheim: VCH-Wiley, 2001.
01Wer Werner, R.F., Wolf, M.M.: Quantum Inf. Comput. **1** (2001) 1.

02Ang Anglin, J.R., Ketterle, W.: Nature (London) **416** (2002) 211.
02Bur Burnett, K., Julienne, P.S., Lett, P.D., Tiesinga, E., Williams, C.J.: Nature (London) **416** (2002) 225.
02Chu Chu, S.: Nature (London) **416** (2002) 206.
02Gre Greiner, M., Mandel, O., Esslinger, T., Hänsch, T.W., Bloch, I.: Nature (London) **415** (2002) 39.
02Hug Hughes, R.J., Nordholt, J.E., Derkacs, D., Peterson, C.G.: New J. Phys. **4** (2002) 43.

02Kie Kiesel, H., Renz, A., Hasselbach, F.: Nature (London) **418** (2002) 392.

02Met Metcalf, H.J., van der Straten, P.: Laser cooling and trapping, New York: Springer-Verlag, 2002.

02Mon Monroe, C.: Nature (London) **416** (2002) 238.

02Rol Rolston, S.L., Phillips, W.D.: Nature (London) **416** (2002) 219.

02Spe Spence, J.C.H.: Nature (London) **418** (2002) 377.

02Ste Stenholm, S.: Phys. Rep. **363** (2002) 173.

02Stu Stucki, D., Gisin, N., Guinnard, O., Ribordy, G., Zbinden, H.: New J. Phys. **4** (2002) 41.

02Ude Udem, T., Holzwarth, R., Hänsch, T.W.: Nature (London) **416** (2002) 233.

03Pit Pitaevskii, L., Stringari, S.: Bose-Einstein Condensation, Oxford: Clarendon Press, 2003.